

ANALYSIS OF THE THREE-PHASE RELUCTANCE
MOTOR

By

ELMAN R. SHOWERS

Bachelor of Science in Electrical Engineering
Oklahoma Agricultural and Mechanical College
Stillwater, Oklahoma

1949

Submitted to the Faculty of the Graduate School of
the Oklahoma Agricultural and Mechanical College
in Partial Fulfillment of the Requirements
for the Degree of
MASTER OF SCIENCE

1951

OKLAHOMA
AGRICULTURAL & MECHANICAL COLLEGE
LIBRARY
JUL 26 1951

ANALYSIS OF THE THREE-PHASE RELUCTANCE
MOTOR

ELMAN R. SHOWERS

MASTER OF SCIENCE

1951

THESIS AND ABSTRACT APPROVED:

Chas. F. Cameron

Thesis Adviser

A. Natter

Faculty Representative

D. B. McIntosh

Dean of the Graduate School

277967

PREFACE

The reluctance motor is one of the very few devices found in electrical machinery about which little has been written. A search into the available sources of information yields small results. In fact the very name is seldom mentioned. Since the reluctance motor operates at relatively low efficiency and power factor, compared to the excited synchronous motors, its application is confined to cases wherein these considerations are of minor importance.

General information about the reluctance motor is given in Chapter I Part I. More specific information about the polyphase reluctance motor is included in Chapter I Part II. Although this thesis is primarily concerned with the polyphase reluctance motor, it was thought desirable to give the reader in Chapter I Part III a brief knowledge of the single-phase reluctance motor due to its widespread use.

This thesis was confined to the polyphase reluctance motor since it lent itself readily for analysis with the available laboratory equipment.

Any synchronous d-c excited salient pole a-c machine will operate on the reluctance principle. Consequently, a three-phase Westinghouse (a-c generator) No. 4,887,398 was chosen as the machine to be tested for operation as a three phase reluctance motor. The results of this test are tabulated and discussed in Chapter IV.

Chapter II gives a magnetic interpretation of the phenomena taking place in the stator and rotor of the reluctance motor.

Theoretical development for predicting the performance of the three-phase reluctance motor composes Chapter III. Great emphasis is based on obtaining an accurate interpretation of fundamental quantities.

Finally, a comparison is made between the results as calculated by the developed theoretical equations and those obtained from the experimental test.

ACKNOWLEDGEMENT

The writer wishes to express his sincere appreciation to Professor C. F. Cameron for his many helpful suggestions and careful scrutiny of this material.

TABLE OF CONTENTS

CHAPTER I	Reluctance Motor	1
PART I	General Information	1
PART II	Polyphase Reluctance Motor	2
PART III	Single Phase Reluctance Motor	5
CHAPTER II	Magnetic Theory	6
PART I	Atomic Structure	6
Figure II-1	Structure of Atom	7
Figure II-2	Gyroscopic and Gyromagnetic Action	8
PART II	Atomic Forces	9
PART III	Crystal Structure	11
PART IV	Magnetic Theory Applied to the Reluctance Motor . .	13
CHAPTER III	Theoretical Development	14
PART I	Basic Quantities	14
Figure III-1	Methods of Inducing Voltage	16
PART II	Examples Showing Agreement or Disagreement Between Equations III-4 and III-5	18
Figure III-2	Rotating Loop	18
Figure III-3	Swinging Conductor	19
PART III	Mathematical Derivation of Equations III-4 and III-5	22
PART IV	Synchronous Machine Concepts	32
Figure III-4	Leakage Inductance-Secondary Open	36
Figure III-5	Leakage Inductance-Secondary Shorted	38
Figure III-6	Direct Synchronous Reactance Flux Paths	46
Figure III-7	Quadrature Synchronous Reactance Flux Paths . . .	48
PART V	Mathematical Analysis of the Three-Phase Reluctance Motor	49
Figure III-8	Synchronous Motor Vector Diagram	50

CHAPTER IV	Experimental Analysis of the Three-Phase Reluctance Motor	53
PART I	Determination of X_d and X_q	53
Figure IV-1	Waveform Oscillogram	56
PART II	Reluctance Motor Performance Test	57
Curve Sheet IV-1	Determination of True Torque Angle	59
Table IV-1	Test Data: Reluctance Motor	60
Curve Sheet IV-2	Torque Angle Versus Output Power	62
Table IV-2	Calculated Data: Reluctance Motor	63
Curve Sheet IV-3	Efficiency and Power Factor Versus Output Power	64
Table IV-3	True Torque Angle Calculation Data	65
Curve Sheet IV-4	Plot of In-phase Current Versus Out-of-phase Current	66
Table IV-4	Calculated Data: Reluctance Motor	67
Table IV-5	Calculated Data: Line Current Components	68
Table IV-6	Calculated Power: Theoretical	69
PART III	Comparison of Theoretical and Experimental Results	70
CONCLUSION	74
BIBLIOGRAPHY	75

CHAPTER I

Reluctance Motor

PART I

General Information

A reluctance motor operates by virtue of a variation in the reluctance of the magnetic path. Since it runs at synchronous speed without any d-c field excitation it is widely used in applications requiring constant speed. Its use in synchronous clocks is only one of many examples.

The reluctance motor starts as an induction motor regardless of whether it is of the single phase or of the polyphase variety. In the case of the small single phase motor the squirrel cage rotor serves as the starting mechanism. Starting is achieved in a similar manner on the larger polyphase motors by utilizing the already present damper windings.

PART II

Polyphase Reluctance Motor

The ordinary salient pole polyphase motor operating at synchronous speed will continue to function if the excitation is removed. When operating in this manner it is known as a reluctance motor. As far as the principle of operation is concerned the stator winding may be any one of a number of standard types. In order to start the motor from standstill, some type of starting winding must be incorporated such as a damper winding, so that the motor may start on the induction motor principle.

Usually the saliency of the rotor is obtained by filing or milling flats on an ordinary squirrel cage rotor. Tests on these machines show that pull-out torque changes very little as a result of cutting the flats. However, the flats greatly increase the cogging tendency and thereby reduce the minimum starting torque. With this type of motor its synchronous pull-out torque is approximately one-third the induction motor pull-out torque. As a result of this, small motors operating under the reluctance principle are rated at only one-half or one-third that obtained when operating as an inductance motor. Usually to obtain a rating as large as one-half the iron parts must be worked much harder.

The speed at which synchronization takes place depends upon the inertia of the rotating mass, i.e. the inertia of the rotor plus that of the load. This may be deduced from the following discussion. An accelerating torque is exerted when the rotor pole passes and lags behind zero to one-half pole pitch of the rotating magnetic field. However, when the rotor pole lags more than one-half but less than one pole pitch of the rotating magnetic field a retarding torque is produced which tends to decelerate

the rotor. While the motor is starting, the squirrel cage or damper winding accelerates the rotor.

When synchronous speed is approached, the salient poles of the rotor slip by the poles of the rotor at a progressively slower speed. During the interval when the rotor pole lags the rotating magnetic field from zero to one-half magnetic pole pitch the rotor must be accelerated enough in order to enable it to reach synchronous speed otherwise it will slip to a position between one-half pole and one pole and immediately be decelerated with a consequent reduction in speed. When continual slipping occurs the average reluctance torque becomes zero. The amount of energy which the reluctance effect must contribute to the rotor in order to affect synchronization is therefore dependent upon the total rotating inertia and the maximum speed which the motor can attain while operating as an induction motor. Since the maximum speed is related to the rotor resistance, the latter is very important in determining whether synchronization may be attained.

In the case of induction motors a low resistance rotor gives maximum torque at low values of slip. Increasing the rotor resistance causes the maximum torque to occur at larger values of slip. If the starting torque is about the same as the full load torque, the rotor resistance should be low enough to provide sufficient torque in order to enable the rotor to approach close to synchronous speed and yet great enough to provide sufficient starting torque. If the required starting torque is high compared to the full load torque, the rotor resistance should be larger than in the previous case.

As would be expected the rotor resistance does not affect the reluctance torque once the rotor poles have locked in with the rotating magnetic

poles. However, for good pull-in torque characteristic, the rotor resistance should be low.

The result of milling the flats on the rotor is to cause a cogging effect. This may be minimized by skewing the flats.

Efficiency and power-factor of the polyphase reluctance motor is slightly less than the performance of the same motor operated as an induction motor at one-third full load.

PART III

Single Phase Reluctance Motor

In the single phase nonexcited synchronous motor the rotors are of the ordinary squirrel cage type with flats milled on them. The total area of the flats is approximately 40 per cent of the total cylindrical area of the rotor before the flats are milled. The rotor resistance rings and the conductors in the flat part are sometimes partially but not entirely removed.

The stator consists of two windings in space quadrature. One winding is used as a starting winding and is connected in series with the centrifugal starting switch and a resistor or capacitor depending upon whether it is of the split-phase or capacitor starting type. Sometimes the starting winding is used with a two value capacitor where both are used for starting and one for running. The remaining winding is used at all times.

As in the case of the polyphase reluctance motor, the single phase reluctance motor develops about one-third as much horsepower as when operating as an induction motor. Cogging tendencies are much greater than in the case of polyphase reluctance motor since the starting torque is so much less. However, for the same reason cogging is not so marked in the two value capacitor motor.

CHAPTER II

Magnetic Theory

PART I

Atomic Structure

An understanding of the present day theory of ferromagnetism is of great help in determining why the polyphase motor is able to operate. Since there is no d-c field excitation, the operation of the motor at synchronous speed can only be explained in terms of the basic concepts of magnetism.

The atom is believed to consist of a nucleus surrounded by planetary electrons. These planetary electrons are found in discrete shells. For iron there are 4 principal shells. There are a maximum of 2, 8, 18, and 32 electrons possible in shells 1-4 respectively where the number one corresponds to the shell closest to the nucleus. In many elements the maximum allowable number of electrons in a shell is not attained before the next outer shell begins filling. The iron atom is one in which not all of its shells are filled. It has 2, 8, 14, and 2 electrons in shells one to four respectively. The periodic system of the elements is formed by beginning with hydrogen, the lightest of elements, and adding planetary electrons in the innermost shell. Refer to Figure II-I to see how many additional electrons are required to form a new element. Notice in particular, that iron is obtained by adding 6 electrons in the third ring of the third shell. Five of these electrons are spinning in a positive direction and the remaining one is spinning in the negative direction. Consequently, there is an unbalance of 4 positive spins. Ferromagnetism is believed to be intimately connected with the building

up of the third shell. If one more planetary electron is added, the iron is transformed into cobalt, and now only 3 excess spins result. Pertinent to the addition of planetary electrons is the simultaneous requirement of adding a positive charge and its associated mass to the nucleus.

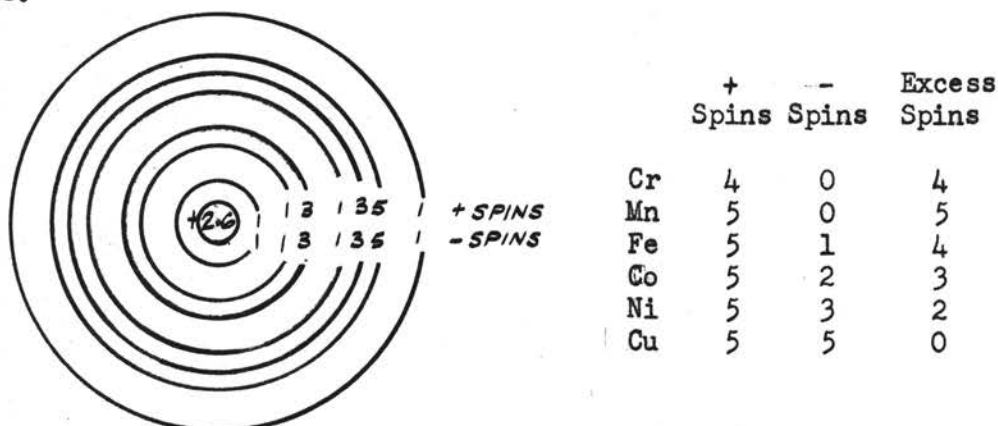
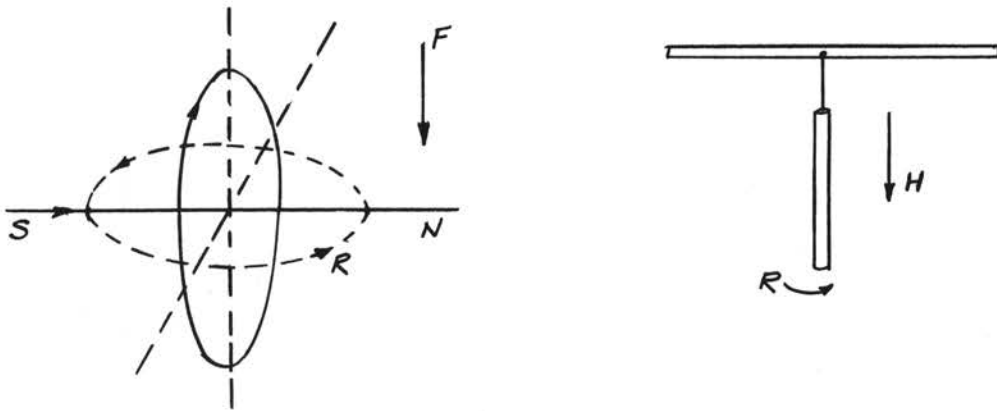


FIGURE II-1

For many years magnetism was believed to be the result of the electrons moving in orbits around the nucleus. However, as a result of observations of spectral lines, the spectroscopists suggested that each electron was also spinning about its own axis. Thus each electron acts as a small gyroscope having a definite magnetic moment on account of its moving electrical charge and a definite angular momentum on account of its mass. The ratio of these two quantities has been found to have a specific value. Due to the orbital motion the electrons possess an additional magnetic moment and angular momentum. However, in this case the ratio is only one-half that in the previous case.

The existence of the magnetic and mechanical moments and the determination of the ratio between them was obtained by the Barnett experiment. This consists of hanging a rod of iron from a fine suspension and suddenly magnetizing the rod. Immediately the rod turns.



Gyroscopic action (left), force F produces rotation R
 Gyromagnetic effect (right), field H produces rotation R

FIGURE II - 2

The explanation is that application of the applied field causes the elementary magnets to be turned more nearly parallel with the axis of the rod, thereby causing the net angular momentum to be parallel to that axis. For stability to ensue, the action must be balanced by an equal and opposite reaction. Hence, the suspension twists, thereby supplying the reaction. From this experiment it may be deduced that a change in magnetism is a result of the change of spin direction and not a change in orientation of the whole electron orbit.

PART II

Atomic Forces

In order for an element to be ferromagnetic, it is necessary that there be uncompensated spins which are parallel in neighboring atoms. If this parallelism is to be attained, it is necessary that the diameter of an atom bear the proper ratio to the diameter of the electron shell which has the uncompensated spins. This follows from the fact that the electron spins and charges influence each other to an amount depending upon the distance between them. This influence is known as the "exchange". In ferromagnetic materials the ratio must be greater than 1.5. The forces of exchange are purely electrostatic in origin since they are the result of electric charges distributed in space in a definite way. The exchange forces act to keep the spins parallel while thermal forces attempt to prevent this alignment. As the temperature is increased the thermal forces increase until a point is reached where they prevail over the exchange forces, thereby causing the material to cease being ferromagnetic. This temperature is known as the Curie point. The height of this point is a measure of the exchange.

The ultimate magnetism or saturation value depends upon the number of excess electron spins and also upon the exchange forces, since this determines the final number of electron spins which can be oriented parallel to the field. Roughly, it may be said to depend upon the product of the exchange and the number of uncompensated spins in the atom. This agrees with the fact that iron-cobalt alloys have a higher saturation value than iron.

The larger the forces of exchange are, the easier it is to align the excess spins of neighboring atoms. In ferromagnetic materials the

exchange forces are so large that spins in small regions are parallel even without the application of an external magnetic field. However, this parallelism does not extend over the whole specimen. Experiments have shown these regions to have the volume of a cube whose edge is about 0.001 inches. This small volume, known as a domain, is magnetized to saturation. Any given specimen would be composed of a great many of these domains. In unmagnetized material the domains are equally oriented in all directions so that the total magnetism is zero.

The existence of these domains has been experimentally verified by the Barkhausen effect. This is done by gradually increasing the magnetic field around the specimen and simultaneously listening to the output of a telephone receiver connected to a coil wound around the specimen. As the field is increased a series of clicks are heard. Each click corresponds to a reversal of magnetism in the cube.

PART III

Crystal Structure

During recent years means for controlling grain size have been developed so that it is now possible to produce single crystals large enough to perform experiments on one such crystal.

In a crystal the atoms are arranged in a regular form. Each atom may be thought of as a small magnet due to the spinning electrons and also to the orbital motion of the electrons. Consequently, some directions of magnetization are more stable than others. For iron the most stable direction is the cube edge, while for nickel it is the cube diagonal.

The electrostatic exchange forces are responsible for lining the spins parallel to each other. However, it is the crystal forces which determine the direction of parallelism. Crystal forces are very weak compared to the exchange forces. As small a field as 1,000 oersteds will redirect the spins of an entire group of atoms. However, in the absence of exchange forces it would take 10,000,000 oersteds to align the spins of a group of atoms.

The unmagnetized crystal consists of domains, all of which are magnetized to saturation. Application of a magnetic field causes a change of direction of magnetization from one stable direction to one most nearly parallel to the direction of applied field, thereby increasing the resultant magnetization in the field direction. From this it may be concluded that portions of the B-H curve are not smooth as ordinarily shown, but if greatly magnified, they would consist of a series of stair steps. Further increase of the magnetic field causes the electron spins in each domain to be rotated out of the stable direction toward the field

direction. This process, known as "rotation of the domain", occurs only in high fields.

Magnetization in very small fields occurs as a result of displacing the boundaries of the domains. Hence in this region, the B-H curve will be smooth even though greatly magnified. A smooth curve also is obtained at high fields when the domains are being rotated.

PART IV

Magnetic Theory Applied to the Reluctance Motor

In the stator of the polyphase reluctance motor the magnetic field is constantly changing due to progressive building up of the currents in some phases while it is decreasing in others. As the mmf. at a given point builds up, at first the boundaries of the domains shift, next the direction of magnetization of the domains is shifted to the direction of easy magnetization most nearly parallel to the applied field, and finally the directions of magnetization of the domains are rotated parallel to the applied field. The inverse process occurs while the applied field decreases to zero.

The phenomena in the rotor differs from that in the stator in that once synchronous speed is attained, the mmf. at any point of the rotor is constant. Consequently, upon applying an mmf. to the rotor iron, only the first part of the previous cycle occurs. In normal operation all domains are magnetized in the direction of easiest magnetization most nearly parallel to the applied field, and if a large enough mmf. is present the domains are also rotated in the direction of applied field. The effect of the applied mmf. on the domains of the rotor is to cause a torque in the direction of the rotating mmf. In order for the magnetic field to create a net torque in a given direction, the reluctance of the magnetic path must be different in different axis directions of the rotor. Otherwise, the sum of the torques over one pole pitch of the rotor periphery is zero. It is the existence of unequal reluctance in different paths that makes it possible for the stator mmf. to produce a net torque in the rotor.

CHAPTER III

Theoretical Development

PART I

Basic Quantities

The theoretical analysis of the reluctance motor will proceed in the following manner: (1) defining the fundamental concepts and (2) developing new relationships by means of mathematics. The latter will be verified by experimental studies in Chapter IV.

Since a clear interpretation of the final results requires a thorough understanding of the fundamental concepts, these will be covered in great detail in this chapter.

The following quantities will be used with units of the practical system.

e - Electromotive force (emf) or voltage

i - Current

t - Time

ϕ - Flux

ψ - Flux linkage

Their respective units are volts, amperes, seconds, lines, and line-turns.

Basically, voltage is the amount of work accomplished in moving a unit positive charge from one point to another. Mathematically, potential difference may be represented as $\int_{P_1}^{P_2} F \cos \theta \, dl$ where F represents the magnitude of vector force \vec{F} and is a function of position, and θ is the angle between vectors \vec{F} and \vec{dl} . Where low frequencies are involved and the space relationships are comparably small, the value of voltage between

two points is independent of the path taken. This is only true when a conservative field exists. That is, the phenomena occurring at one point is not influenced by that occurring at some other point for a different instant of time. Note that this is not to be confused with phase angle displacement of vectors, for this is merely a means of denoting time variation between the occurrence of the peak values (or some other periodically occurring values).

Current, i , is defined by $\frac{dq}{dt}$ where q is the charge in coulombs and t is the time in seconds.

Flux linkage, ψ , is the summation of the product of each flux line and the number of turns it links, or the summation of the number of flux lines linking each turn. This may be expressed as

$$\text{III-1} \quad \psi = \sum_{q=0}^K N_q \psi_q \quad \text{or}$$

$$\text{III-2} \quad \psi = \sum_{p=0}^K N_p \psi_p$$

where, in equation III-1, q is the flux line number and N_q is the number of turns linked by the q^{th} flux line; and in equation III-2, where p is the turn number and ψ_p is the number of flux linking the p^{th} turn.

Faraday's law, the law of induction, states that a voltage is induced in a conduction wire equal to the total number of magnetic flux lines cut per second. If the wire is so arranged as to consist of n identical elements, such as a bundle of n turns, the statement can be modified to read that the voltage is equal to the total flux cut multiplied by the number of turns. If we define ϕ to be the total magnetic flux, then $\phi = \int \bar{B} \cdot \bar{da}$ where \bar{B} is the magnetic flux density. Faraday's law is, therefore

$$\text{III-3} \quad e = -n \frac{d\phi}{dt} = -n \frac{d}{dt} (\bar{B} \cdot \bar{da})$$

A close scrutiny of equation III-3 shows that a voltage may be induced into a circuit in a variety of ways. Figure III-1 illustrates three simple ways, each of which represents varying a different part of equation III-3. Figure III-1a represents a transformer in which the current I produces a magnetic flux through the iron core varying, say, sinusoidally with time. The voltage V will also vary sinusoidally 90° out of phase with the current I . A voltage induced in this way is called voltage by transformer action.

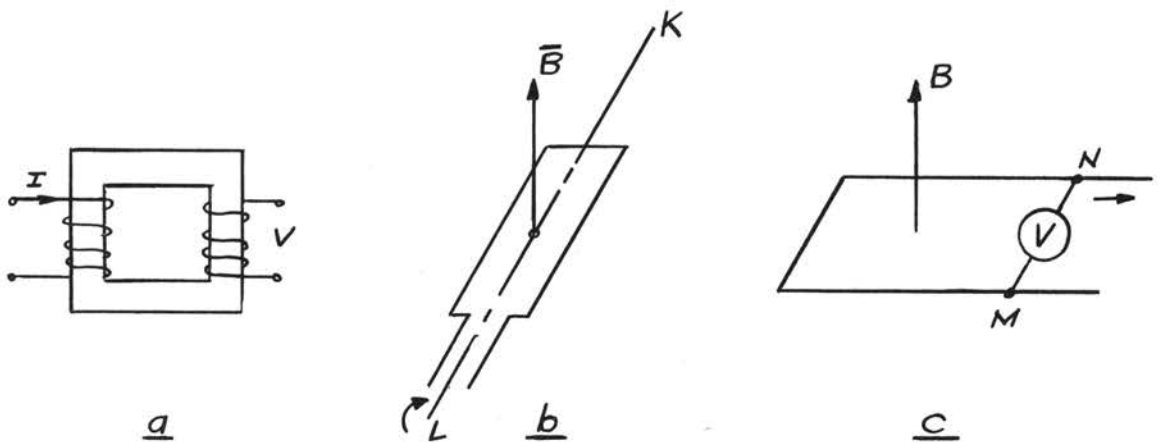


Figure III-1

Figure III-1b represents an alternating current generator in which a voltage is induced by a change in the angle between magnetic flux and a vector representation of the area. In Figure III-1b, \vec{B} is a constant vector but the wire loop is permitted to rotate about the axis KL . Since a cosine of the angle between \vec{B} and each element $d\vec{a}$ varies sinusoidally if the angular motion is constant, the voltage induced in the winding varies sinusoidally with time. The voltage induced in this case is called a motional voltage. Figure III-1c represents a third method of inducing voltage. It corresponds to varying the limits of the integral in equation

III-3. Here the magnetic flux density is also constant but the segment of wire MN is permitted to slide along the remaining wire, say, sinusoidally. The flux cut by this segment results in an induced voltage which varies sinusoidally with time. Figure III-1c also represents motional voltage. Obviously, combinations of the two types of induced voltage are possible. Such is the case in motors and generators.

PART II

Examples Showing Agreement or Disagreement Between
Equations III-4 and III-5

Induced voltage is defined in two different manners:

$$\text{III-4} \quad e = Bvl \quad \text{or} \quad \text{III-5} \quad e = - \frac{d\phi}{dt}$$

where v , l , and ϕ represent respectively the velocity, length, and magnetic flux.

The above definitions are usually thought of as alternative methods of expressing the same relationship. A very simple example which gives the same induced voltage by either method is the rotating loop in a constant magnetic field.

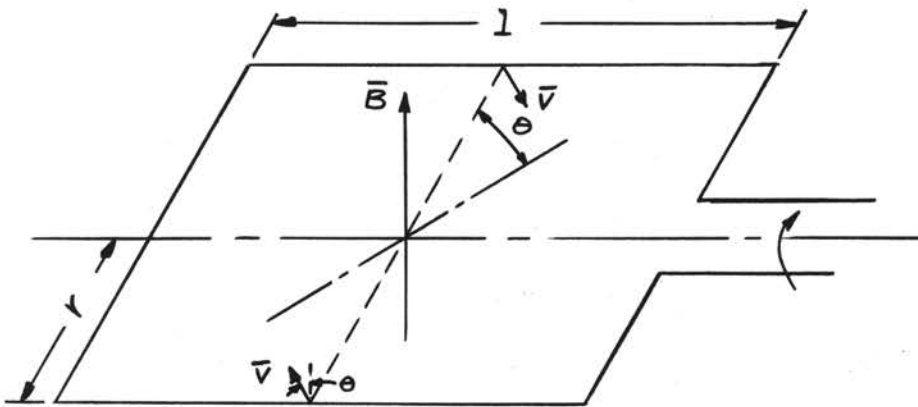


Figure III-2

Using equation III-4, $e = Bvl \sin\theta$, gives

$$e = 2Bvl \sin\theta.$$

And by using equation III-5, $e = - \frac{d\phi}{dt}$, gives

$$e = -B \frac{d}{dt} (2lv \cos\theta)$$

$$= 2Blv \frac{d\theta}{dt} \sin\theta,$$

but $r \frac{d\theta}{dt} = v$, therefore $e = + 2Bvl \sin\theta.$

Consequently, as a result of this common example, both laws are believed to give the same results in all cases. Actually, there are many examples in which different results are obtained by the two methods.

The following example serves to illustrate one of many cases in which equations III-4 and III-5 do not give the same answers. Figure III-3 shows a conductor swinging back and forth from the pivot points a-a' through a small enough angle so that the motion is essentially horizontal. The velocity of the conductor is $v = v_m \cos \omega t$. A time varying current is applied to the field winding so that the flux density follows the relationship $B = B_m \cos \omega t$. The flux is upward and the conductor is moving toward the right when the function $\cos \omega t$ is positive. Consequently, it would seem that a voltage of constant direction but varying magnitude would be induced in the conductor. For this reason, this device is erroneously called the d-c generator without moving contacts.

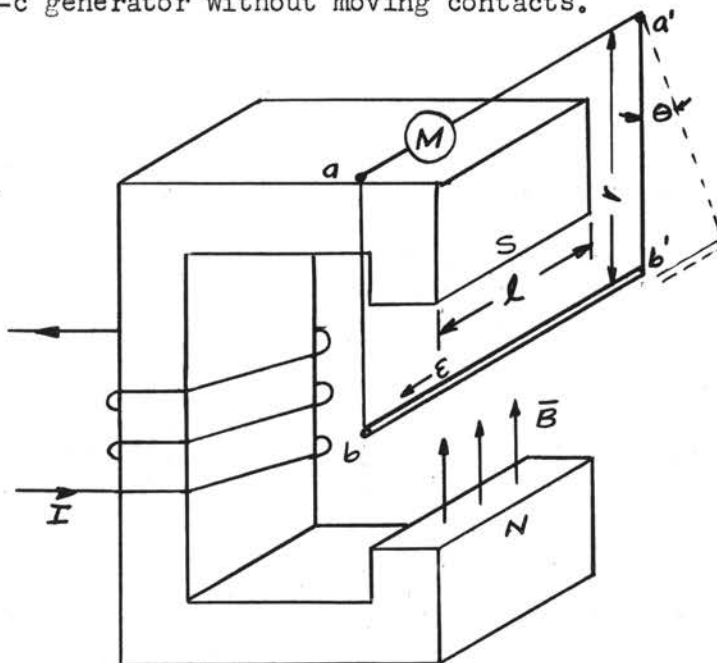


Figure III-3

By using equation III-5, the flux linking law, a result is obtained which is identical to that obtained by experimental means. Derived in the following manner, it is

$$\begin{aligned} e &= \frac{d\phi}{dt} \\ &= \frac{d}{dt} (\bar{A} \cdot \bar{B}) \end{aligned}$$

where \bar{A} is the area of a rectangle, the sides of which are l and $r \cos \theta$. The plus sign is used in place of the minus sign so that the direction of e is consistent for all three methods.

By setting the horizontal velocity function in terms of ωt equal to that obtained in terms of $\frac{d\theta}{dt}$ (for small angles) and integrating the result, the value of $\theta = \frac{v_m}{\omega r} \sin \omega t$ or $\theta = \sin \omega t$ is obtained. By substituting these values, the expression for the induced voltage becomes

$$\begin{aligned} e &= \frac{d}{dt} \left[(lr \theta) (B_m \cos \omega t) \right] \\ &= \frac{d}{dt} \left[B_m lr (\cos \omega t) \sin \omega t \right] \\ &= B_m lr \omega (\cos^2 \omega t - \sin^2 \omega t) \\ \text{III-6} \quad &= B_m v_m l \cos 2 \omega t \end{aligned}$$

Now by using equation III-4, the flux cutting law, gives

$$\begin{aligned} e &= \bar{v} \times \bar{B} \cdot \bar{l} \\ &= v_m (\cos \omega t) (B_m \cos \omega t) l \\ &= B_m v_m l \cos^2 \omega t \\ \text{III-7} \quad &= 1/2 B_m v_m l + 1/2 B_m v_m l \cos 2 \omega t \end{aligned}$$

which is different than that previously obtained.

However, if Maxwell's equation for transformer induction is used and the results added to those obtained by using equation III-4, the same value through use of equation III-5 is obtained. This is obtained as follows:

By Maxwell's equation for transformer induction

$$e = - \iint \frac{\partial \bar{B}}{\partial t} \cdot d\bar{s}$$

By making the appropriate substitutions and integrating

$$e = -1/2 B_m v_m l - 1/2 B_m v_m l \cos 2 t$$

Adding equations III-7 and III-8 gives

$$\begin{aligned} e &= B_m v_m l (1/2 - 1/2 \cos 2 t) - (-1/2 - 1/2 \cos 2 t) \\ &= B_m v_m l \cos 2 t \end{aligned}$$

In some cases the results experimentally determined verify (1) equation III-4, the flux cutting law, (2) equation III-5, the flux linking law, (3) the sum of equations III-4 and III-5, and (4) neither (1) nor (2) nor the sum.

PART III

Mathematical Derivation of Equations III-4 and III-5

The intelligent application of formulas III-4 and III-5 requires additional information in order to assure obtaining the correct answer to any specific problem. Therefore, the two will be derived, thus showing their limitations. For simplification the mks. system of units will be used herein.

It can be experimentally shown that charges at rest exert a force on each other as a result of their position. This is expressed differentially in the mathematical form as

$$\text{III-8} \quad d^2\vec{F}_1 = \frac{dq_1 dq_2 \vec{r}}{4\pi\epsilon r^3}$$

where $d^2\vec{F}_1$ is the differential force exerted on charge dq_1 by charge dq_2 .

Also, if two charges are moving, there is a force exerted upon each other as a result of these velocities which is

$$\text{III-9} \quad d^2\vec{F}_1 = \frac{\mu dq_1 dq_2 \vec{v}_1 \times (\vec{v}_2 \times \vec{r})}{4\pi r^3}$$

where \vec{v}_1 and \vec{v}_2 are the velocities of dq_1 , and dq_2 respectively.

Furthermore, charges experience forces due to being accelerated equal to the value

$$\text{III-10} \quad d^2\vec{F}_1 = \frac{-\mu dq_1 dq_2 \vec{a}_2}{4\pi r}$$

where μ is the permeability and \vec{a}_2 the acceleration of dq_2 .

In the case of the conducting wires, the charges are comparatively concentrated, residing on the wire and hence, since current represents flow of charges past a point per time, multiplying it by length gives the velocity at which the charge flows.

$$I = \frac{dq}{dt} \quad \text{multiplying both sides by } \overline{dl}, \text{ gives}$$

$$I \overline{dl} = \frac{dq}{dt} \overline{dl} \quad \text{rearranging}$$

$$I \overline{dl} = dq \frac{\overline{dl}}{dt} = dq \overline{v} \quad \text{or}$$

$$\text{III-11} \quad \overline{v} = \frac{I \overline{dl}}{dq} \quad \text{and} \quad \text{III-12} \quad dq = \frac{I \overline{dl}}{\overline{v}}$$

This value of dq may be substituted in the force equations involving motion, thereby giving

$$\text{III-13} \quad \frac{d^2 F_1}{dt^2} = \frac{\mu I_1 I_2 \overline{dl}_1 \times (\overline{dl}_2 \times \overline{r})}{4\pi r^3}$$

Similarly the acceleration becomes

$$\frac{d^2 F_1}{dt^2} = -\frac{\mu dq_1 dq_2 \overline{a}_2}{4\pi r}$$

since $\frac{d\overline{v}}{dt} = \overline{a} = \frac{\partial I}{\partial t} \frac{\overline{dl}}{dq}$

Note that \overline{dl} is a function of distance and not time.

$$\begin{aligned} &= -\frac{\mu dq_1 dq_2}{4\pi r} \frac{\partial I_2 \overline{dl}_2}{\partial t dq_2} \\ \text{III-14} \quad &= \frac{-\mu dq_1 \overline{dl}_2}{4\pi r} \frac{\partial I_2}{\partial t} \end{aligned}$$

Since this analysis is to cover a range of frequencies in which the physical system is small in comparison to a wavelength, forces on charges due to radiation effects will be neglected.

Equations of the three type of fields which cause a force on charges, namely (a) electrostatic field, (b) Magnetic field, and (c) Vector-potential field are as follows:

$$\text{III-15} \quad d\overline{E} = \frac{dq_2 \overline{r}}{4\pi \epsilon r^3}$$

$$\text{III-16} \quad d\bar{B} = \frac{\mu \, dq_2 \, \bar{v}_2 \times \bar{r}}{4\pi r^3}$$

$$\text{III-17} \quad d\bar{A} = \frac{\mu \, dq_2 \, \bar{v}_2}{4\pi r}$$

Using the same relation $I \, d\bar{l} = \bar{v} \, dq$ and substituting for \bar{v}_2 , gives

$$\begin{aligned} d\bar{B} &= \frac{\mu \, dq_2 \, \frac{I_2 d\bar{l}_2}{dq_2} \times \bar{r}}{4\pi r^3} \\ \text{III-18} \quad &= \frac{\mu \, I_2 \, d\bar{l}_2 \times \bar{r}}{4\pi r^3} \end{aligned}$$

and

$$\begin{aligned} d\bar{A} &= \frac{\mu \, dq_2}{4\pi r} \left[\frac{I_2 d\bar{l}_2}{dq_2} \right] \\ \text{III-19} \quad &= \frac{\mu \, I_2 \, d\bar{l}_2}{4\pi r} \end{aligned}$$

The force formulas may now be expressed in terms of the electrostatic, electromagnetic, and vector potential fields.

$$d^2F_1 = \frac{dq_1 \, dq_2 \, \bar{r}}{4\pi\epsilon r^3}$$

$$\text{Substituting} \quad d\bar{E}_s = \frac{dq_2 \, \bar{r}}{4\pi\epsilon r^3} \quad \text{gives}$$

$$\text{III-20} \quad d^2F_1 = dq_1 \, d\bar{E}_s \quad \text{and integrating results in}$$

$$dF_1 = \int dq_1 \, d\bar{E}_s$$

$$\text{III-21} \quad = dq_1 \, \bar{E}_s$$

Similarly

$$d^2\bar{F}_1 = \frac{\mu \, dq_1 \, dq_2 \, \bar{v}_1 \times (r_2 \times r)}{4\pi r^3}$$

$$\text{Substitute} \quad d\bar{B} = \frac{\mu \, dq_2 \, \bar{v}_2 \times \bar{r}}{4\pi r^3}$$

$$\text{III-22} \quad d^2\bar{F}_1 = dq_1 \bar{v}_1 \times d\bar{B}$$

$$\begin{aligned} \text{Integrate once} \quad d^2\bar{F}_1 &= \int dq_1 \bar{v}_1 \times d\bar{B} \\ &= dq_1 \int \bar{v}_1 \times d\bar{B} \end{aligned}$$

$$\text{III-23} \quad = dq_1 \bar{v}_1 \times \bar{B}$$

$$\text{Likewise} \quad d^2F_1 = \frac{-u dq_1 dq_2 \bar{a}_2}{4\pi r}$$

$$\begin{aligned} \text{Since} \quad d\bar{A} &= \frac{u dq_2 \bar{v}_2}{4\pi r} \\ \frac{\partial(d\bar{A})}{\partial t} &= \frac{u dq_2}{4r} \frac{\partial \bar{v}_2}{\partial t} \end{aligned}$$

$$\text{III-24} \quad = \frac{u dq_2}{4\pi r} \bar{a}_2$$

Substitute in formula

$$\text{III-25} \quad d\bar{F}_1 = -dq_1 \frac{\partial(d\bar{A})}{\partial t}$$

$$\begin{aligned} \text{Integrating gives} \quad d\bar{F}_1 &= -\int dq_1 \frac{\partial(d\bar{A})}{\partial t} \\ &= -dq_1 \frac{\partial}{\partial t} \left[\int d\bar{A} \right] \end{aligned}$$

$$\text{III-26} \quad = -dq_1 \frac{\partial \bar{A}}{\partial t}$$

The total force exerted on the charged particle by virtue of its position, velocity, and acceleration will be the sum of the respective forces associated with each.

$$\text{III-27} \quad dF_1 = dq_1 \bar{E}_s + dq_1 \bar{v}_1 \times \bar{B} - dq_1 \frac{\partial \bar{A}}{\partial t}$$

$$\text{III-28} \quad = dq E_{eq}.$$

$$\text{Where} \quad E_{eq} = \bar{E} + \bar{v}_1 \times \bar{B} - \frac{\partial \bar{A}}{\partial t}$$

$$= \bar{E}_s + \bar{E}_m + E_t$$

and \bar{E}_s is the electrostatic field

$$\text{III-29} \quad \bar{E}_m = \bar{v}_\perp \times \bar{B}$$

the equivalent electric field which would cause the same force on dq_\perp as the magnetic field.

$$\text{III-20} \quad E_t = -\frac{\partial \bar{A}}{\partial t}$$

the equivalent electric field which would cause the same force on dq as the vector potential field.

If dq_\perp is a unit charge the total force becomes

$$\begin{aligned} \text{III-31} \quad \bar{F} &= \bar{E}_s + \bar{v}_\perp \times \bar{B} - \frac{\partial \bar{A}}{\partial t} \\ &= \left[\bar{E}_s - \frac{\partial \bar{A}}{\partial t} \right] + \bar{v}_\perp \times \bar{B} \end{aligned}$$

This is known as the Lorentz force formula for a unit charge.

\bar{E}_s is the electrostatic field given by

$$\bar{E}_s = -\text{gradient of } \psi$$

where ψ is the scalar potential

Transformer Induction

Induced voltage caused by pure transformer action, that is absence of motion, is equal to the negative partial derivative of the vector field.

$$\text{III-32} \quad E_t = -\frac{\partial A}{\partial t}$$

Vector potential fields and magnetic fields are related by the following expression

$$\text{III-33} \quad \bar{B} = \nabla \times \bar{A}$$

where \bar{B} is the magnetic density flux vector.

If the curl is taken of both sides of the equation

$$\text{III-32} \quad \nabla \times \bar{E}_t = \nabla \times \left(- \frac{\partial \bar{A}}{\partial t} \right)$$

$$\nabla \times \bar{E}_t = - \frac{\partial}{\partial t} (\nabla \times \bar{A})$$

$$\nabla \times \bar{E}_t = - \frac{\partial \bar{B}}{\partial t}$$

This is Maxwell's differential formula corresponding to Faraday's induction law.

Stoke's theorem states that if s is a surface in three dimensions having a closed curve C as its boundary, then the circulation of a vector \bar{V} around C is equal to the flux of the curl of \bar{V} over S . When stated mathematically this becomes

$$\text{III-34} \quad \iint_s \bar{n} \cdot (\nabla \times \bar{v}) \, ds = \oint_c \bar{v} \cdot d\bar{r}$$

Where \bar{n} is the unit vector normal to s on that side of s which is arbitrarily taken as the positive side. The positive direction along c is then defined along which an observer traveling on the positive side of s would proceed in keeping the enclosed area to his left.

Changing the variables to those used in the foregoing discussion

$$\text{III-35} \quad \iint_s \bar{n} \cdot (\nabla \times \bar{E}_t) \, ds = \oint_c \bar{E}_t \cdot d\bar{l}$$

Substituting:

$$\iint_s \bar{n} \cdot \left(- \frac{\partial \bar{B}}{\partial t} \right) \, ds = \oint_c \bar{E}_t \cdot d\bar{l}$$

$$\text{III-36} \quad \oint_c \bar{E}_t \cdot d\bar{l} = - \iint_s \frac{\partial \bar{B}}{\partial t} \cdot d\bar{s} \quad \text{when } d\bar{s} = \bar{n} \, ds$$

The voltage generated in a closed loop by transformer action is thus equal to the integral of the negative time derivative over the surface enclosed by the loop.

Since the voltage induced by transformer action is $\mathcal{E}_t = \int \bar{E}_t \cdot d\bar{l}$ substituting $\bar{E}_t = -\frac{\partial \bar{A}}{\partial t}$ gives $\mathcal{E}_t = \int -\frac{\partial \bar{A}}{\partial t} \cdot d\bar{l}$ in terms of the vector potential field. Note that this formula applies for any circuit element and is not restricted by the closed requirement.

Equation III-36 may be written:

$$\text{III-37 } \mathcal{E}_t = -\iint \frac{\partial \bar{B}}{\partial t} \cdot d\bar{s}$$

if we remember that this induced voltage applies only to essentially closed loops.

Motional Induction

Pure motional induction occurs when there is no variation of the magnetic field with respect to time. This case is expressed by:

$$\text{III-38 } \bar{E}_m = \bar{v} \times \bar{B}$$

Similar to before the induced voltage is the line integral of E_m .

$$\begin{aligned} \mathcal{E}_m &= \int \bar{E}_m \cdot d\bar{l} \\ \text{III-39 } \mathcal{E}_m &= \int \bar{v} \times \bar{B} \cdot d\bar{l} \end{aligned}$$

At this point it might be well in reviewing that two formulas have been developed for induced voltage;

- (1) that which expresses induced voltage as a function of a time variation of the vector field while there is no motion.
- (2) that which expresses induced voltage as a function of motion while there is no time variation of the magnetic field.

By combining the two formulas together, one would be obtained which would cover the more general type usually found in the problems of today, i.e. both motional and transformer induced voltage.

Addition of equation III-29 and III-30 gives

$$\text{III-40} \quad \mathbf{E} = \mathbf{E}_m + \mathbf{E}_t = \bar{\mathbf{v}} \times \bar{\mathbf{B}} - \frac{\bar{\mathbf{A}}}{t}$$

The total electromotive force would be the line integral between points a and b, or

$$\begin{aligned} \mathcal{E} &= \int_a^b (\mathbf{E}_m + \mathbf{E}_t) \cdot d\bar{\mathbf{l}} \\ &= \int_a^b \left(\bar{\mathbf{v}} \times \bar{\mathbf{B}} - \frac{\partial \bar{\mathbf{A}}}{\partial t} \right) \cdot d\bar{\mathbf{l}} \\ \text{III-41} \quad &= \int_a^b \bar{\mathbf{v}} \times \bar{\mathbf{B}} \cdot d\bar{\mathbf{l}} - \int_a^b \frac{\partial \bar{\mathbf{A}}}{\partial t} \cdot d\bar{\mathbf{l}} \end{aligned}$$

Now if the line integral is taken around a closed path the formula for induced voltage becomes

$$\text{III-42} \quad \mathcal{E} = \oint \bar{\mathbf{v}} \times \bar{\mathbf{B}} \cdot d\bar{\mathbf{l}} - \oint \frac{\partial \bar{\mathbf{A}}}{\partial t} \cdot d\bar{\mathbf{l}}$$

Applying Stoke's theorem and the relation between the magnetic field density and the vector field gives:

$$\begin{aligned} \mathcal{E} &= \oint \bar{\mathbf{v}} \times \bar{\mathbf{B}} \cdot d\bar{\mathbf{l}} - \iint \nabla \times \frac{\bar{\mathbf{A}}}{t} \cdot d\bar{\mathbf{s}} \\ &= \oint \bar{\mathbf{v}} \times \bar{\mathbf{B}} \cdot d\bar{\mathbf{l}} - \iint \frac{\partial}{\partial t} (\nabla \times \bar{\mathbf{A}}) \cdot d\bar{\mathbf{s}} \\ \text{III-43} \quad &= \oint \bar{\mathbf{v}} \times \bar{\mathbf{B}} \cdot d\bar{\mathbf{l}} - \iint \frac{\partial \bar{\mathbf{B}}}{\partial t} \cdot d\bar{\mathbf{s}} \end{aligned}$$

Again applying Stokes theorem to the first term of expression III-41:

$$\begin{aligned} \mathcal{E} &= \iint_s \nabla \times (\bar{\mathbf{v}} \times \bar{\mathbf{B}}) \cdot d\bar{\mathbf{s}} - \iint_s \frac{\partial \bar{\mathbf{B}}}{\partial t} \cdot d\bar{\mathbf{s}} \\ \text{III-44} \quad &= \iint_s \left[\frac{\partial \bar{\mathbf{B}}}{\partial t} - \nabla \times (\bar{\mathbf{v}} \times \bar{\mathbf{B}}) \right] \cdot d\bar{\mathbf{s}} \end{aligned}$$

$$\frac{d}{dt} \iint \bar{B} \cdot d\bar{s} = \iiint \left[\frac{\partial \bar{B}}{\partial t} + \bar{v} \nabla \cdot \bar{B} - \nabla \times (\bar{v} \times \bar{B}) \right] \cdot d\bar{s}$$

Now $\nabla \cdot \bar{B} = 0$ since the divergence of a curl is zero and

$$\nabla \cdot \bar{B} = \nabla \cdot \nabla \times \bar{A} = 0 \quad \text{therefore}$$

$$\frac{d}{dt} \iint \bar{B} \cdot d\bar{s} = \iiint \left[\frac{\partial \bar{B}}{\partial t} - \nabla \times (\bar{v} \times \bar{B}) \right] \cdot d\bar{s}$$

substituting this value in formula III-42 gives:

$$\mathcal{E} = - \frac{d}{dt} \iint \bar{B} \cdot d\bar{s}$$

$$\phi = \iint \bar{B} \cdot d\bar{s} \quad \text{thus:}$$

III-45 $\mathcal{E} = - \frac{d\phi}{dt}$ which is the form of Faraday's flux linking law.

To determine the limitations of the combined formula the first integral term will be examined.

$$\text{III-46} \quad \int_m^b \bar{B} \cdot \bar{r} \times d\bar{l}$$

The term $\bar{r} \times d\bar{l}$ is the differential area swept out per unit time by an element of the circuit. Consequently motion which results in inducing an emf. changes the path of integration. The path of integration must be taken as moving with the material substance composing it, otherwise the electric fields experienced by the changed particles of the material will not be the same as the electric fields taken in the integration. That is, the motion of the paths of integration must be identical with the motion of the material comprising this path at the instant considered.

The combined induction formula or flux linking formula is thus applicable to all closed circuits of constant or changing shape, moving in any

way through a constant or variable changing magnetic field, provided that the motion of every element of the paths of integration is identical with the motion of the matter comprising that path at the instant considered.

As a result of the foregoing derivations, Faraday's Law accounts for all the induced emf. in a closed circuit. This is equivalent to saying that the observer and circuit must be in the same inertia system. An example of the latter would be a voltmeter attached to the circuit either by a fixed connection or sliding contacts such as slip rings but not by a commutator. For in the latter case, the observer is changing his viewing point every time a different coil is brought into the circuit. Consequently, Faraday's law does not express all the induced emf. since there is an additional motional effect between the circuit and the observer's inertial system. This is not to be confused with the velocity of the circuit relative to the field flux. To avoid erroneous results, equations hereafter will always be set up so that the circuit is fixed relative to the observer.

PART IV

Synchronous Machine Concepts

Self inductance may be defined as the constant of proportionality between the flux linkages and the current producing them. In linear circuits the inductance has a constant value and conversely in non-linear circuits it varies with the magnitude of current. Iron circuits show a decrease of inductance with increase of current.

An analogous quantity, mutual inductance, may likewise be defined as the flux linkages in one circuit produced by the current in another circuit. Mathematically expressed, they are:

$$\text{III-47} \quad L = \frac{\psi}{i} 10^{-8} \text{ henrys}$$

and

$$\text{III-48} \quad {}^{\pm} M_{ab} = \frac{\psi_{ab}}{i_b} 10^{-8} \text{ henrys}$$

where the \pm sign of the M depends upon the geometry relating the relative positions of the circuits, and the first subscript of ψ refers to the circuit in which the voltage is induced and the second refers to the circuit in which the current flows.

Simple manipulation gives

$$\text{III-49} \quad \psi = L i \times 10^8$$

and

$$\text{III-50} \quad \psi_{ab} = {}^{\pm} M i_b 10^8$$

substitution in Faraday's law results in

$$\text{III-51} \quad e = -\frac{d(Li)}{dt} \text{ volts}$$

$$\text{III-52} \quad e_a = \frac{d(\pm M_{ab} i_b)}{dt}$$

If L and M are constant with respect to current, it would seem proper to treat them as constants with respect to time and therefore move them outside the differentiation operation indicated. This is a valid operation in stationary circuits involving no motion in themselves or materials composing the conducting paths. Therefore in this case $e = -L \frac{di}{dt}$ or $L = -\frac{e}{\frac{di}{dt}}$. However, in rotating machinery, circuits move relative to each other, and the magnetic circuits are constantly varying; hence L and M may not be treated as constants in this case.

It becomes apparent that when inductance is defined as the ratio of flux linkages to the current producing them, its magnitude is a function of the geometrical configuration of the element wherein the current flows, and of the magnetic circuit. Changing the number of turns, the type of winding, the size or shape of the magnetic path will change the inductance. Furthermore, any change in the magnetic material would change the constant of proportionality.

Both of these effects are taken into account by defining a quantity called permeance, \mathcal{P} , as the ratio of the flux to the magnetomotive force (mmf.) producing it.

$$\text{III-53} \quad \mathcal{P} = \frac{\phi}{.4\pi N^2 I}$$

where $.4 NI$ is the mmf. in practical units. Multiplying numerator and denominator by N gives

$$\text{III-54} \quad \mathcal{P} = \frac{N\phi}{.4\pi N^2 I}$$

$N\phi$ would mean that each turn was linked by all the flux caused by current I .

Normally fractional linkage occurs instead, so that permeance is better defined as

$$\text{III-55} \quad \mathcal{P} = \frac{\psi}{.4\pi N^2 I}$$

where ψ is the same as previously used; i.e. the total number of flux linkages.

The following relationships will be used where prime marks refer quantities to the primary:

$$e_2' = n e_2$$

$$i_2' = n \psi_2 \approx \frac{N_1}{N_2} (N_2 \phi_2) = N_1 \phi_2$$

$$i_2' = i_2 / n$$

$$L_2' = n^2 L_2 = 0.4 \pi 10^{-8} N_1^2 \mathcal{P}_2$$

$$M' = nM = 0.4 \cdot 10^{-8} N_1^2 \mathcal{P}_2$$

$$\text{where } n = \frac{N_1}{N_2} \quad \frac{\text{primary turns}}{\text{secondary turns}}$$

Case I. Primary leakage reactance with secondary open.

Since the resistance of transformers or machine windings has little effect at frequencies of 60 cycles it will be neglected here.

If a sinusoidal voltage of angular frequency ω is applied to the primary, the induced voltage equation requires that

$$\text{III-56} \quad e = - \frac{d\psi}{dt} \cdot 10^{-8}$$

The sinusoidal voltage may be written in the form $e = E e^{j\omega t}$, where e

is understood to be the projection of a rotating vector upon the vertical axis. Substitution gives

$$\text{III-57} \quad E e^{J\omega t} = - \frac{d\psi}{dt} 10^{-8}$$

To solve the above equation assume that $\psi(t) = A e^{J\omega t}$ then substituting gives

$$\text{III-58} \quad E e^{J\omega t} = -A J \omega e^{J\omega t} 10^{-8} \quad \text{or}$$

$$\text{or} \quad E = -A J \omega 10^{-8} \quad \text{or}$$

$$\text{or} \quad \text{III-59} \quad A = \frac{-E}{J\omega} 10^8$$

The homogeneous solution of the induced voltage equation is zero; therefore, the complete solution consists only of the particular solution.

$$\psi(t) = \frac{EJ}{\omega} 10^8 e^{J\omega t}$$

This equation contains the resultant flux corresponding to both a sine and cosine voltage. To obtain that flux resulting from the sine voltage the imaginary part of the right hand expression must be taken.

$$\begin{aligned} \text{III-60} \quad \psi(t) &= \text{Im} \left[\frac{EJ}{\omega} 10^8 e^{J\omega t} \right] \\ &= \frac{E 10^8}{\omega} \text{Im} [J \cos \omega t - \sin \omega t] \end{aligned}$$

$$\text{III-61} \quad = \frac{E 10^8}{\omega} \cos \omega t$$

This may be written in polar form where the relationship between peaks of the flux and applied voltage is indicated.

$$J\bar{\psi} = \frac{E}{\omega} 10^8 \quad \text{or}$$

$$\text{or} \quad \text{III-62} \quad E = J\omega \bar{\psi}$$

$$\text{III-63} \quad E_1 = J\omega \psi_1$$

$$E'_2 = j\omega \bar{\psi}'_2$$

where $\bar{\psi}_1 = \bar{\psi} \cdot 10^{-8}$ and $\bar{\psi}'_2 = \bar{\psi}' \cdot 10^{-8}$

Since $\psi_1(t) = L_1 i_1(t)$ or $\bar{\psi}_1 = L_1 I_1$,

and $\psi'_2(t) = M' i_1(t)$ or $\bar{\psi}'_2 = M' I_1$,

then

$$\text{III-64} \quad E_1 = j\omega L_1 I_1$$

$$\text{III-65} \quad E'_2 = j\omega M' I_1$$

The nonuseful flux linkages which were previously defined are

$$\text{III-66} \quad \psi_1 - \psi'_2 = (L_1 - M') i_1$$

Consequently the leakage inductance under open circuit conditions when referred to the primary is

$$\text{III-67} \quad l_{oc} = L_1 - M'$$

and the leakage reactance is

$$\text{III-68} \quad X_{oc} = \omega (L_1 - M')$$

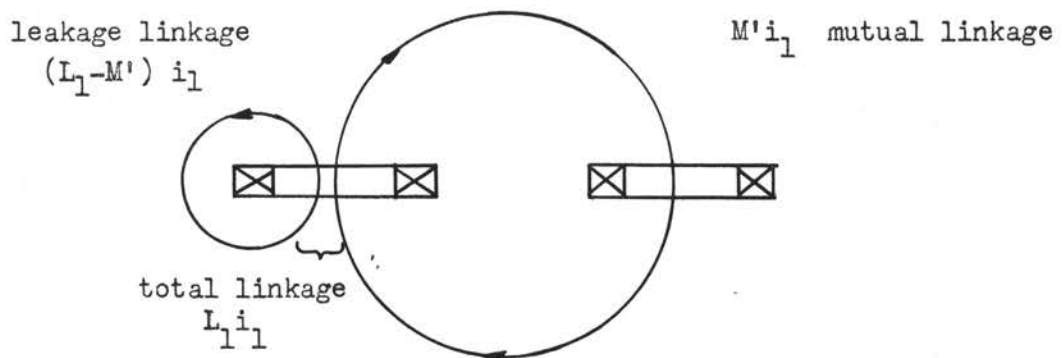


FIGURE III-4

In like manner if the primary were open and the secondary excited, the leakage inductance referred to the primary would be

$$L_2' - M'$$

Case II. Primary excited and secondary short circuited.

In an analogous manner to that for Case I, the differential equation is set up by applying Kirchhoff's voltage law as pertaining to instantaneous values and then solved. This results in the following equations:

$$\text{III-69} \quad E_1 = J\omega \bar{\psi}_1 = J\omega(L_1 I_1 - M' I_2')$$

$$\text{III-70} \quad 0 = J\omega \bar{\psi}_2' = J\omega(L_2' I_2' - M' I_1)$$

By proper choice of currents M has a negative value.

With this convention positive i_1 produces positive ψ_1 and negative ψ_2 , and positive i_2 produces positive ψ_2 and negative ψ_1 .

Solving equations III-70 for I_2 and substituting its value in equation III-69 gives

$$\text{III-71} \quad E_1 = J\omega \bar{\psi}_1 = J\omega \left(L_1 - \frac{M'^2}{L_2} \right) I_1$$

therefore

$$\text{III-72} \quad \bar{\psi}_1 = \left(L_1 - \frac{M'^2}{L_2} \right) I_1$$

$$\bar{\psi}_2' = 0$$

since equation III-70 must hold for all values of ω .

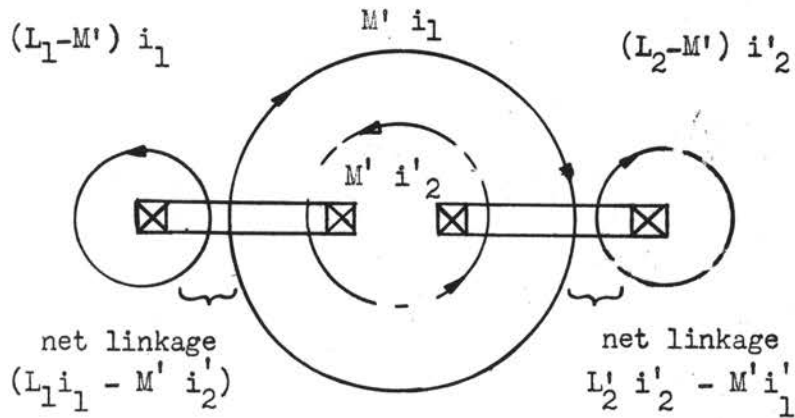


FIGURE III-5

As before leakage linkage is $\psi_1 - \psi'_2$ or $\psi_1 - 0 = \psi_1$. The leakage inductance is then

$$\text{III-73} \quad l_{sc} = \left(L_1 - \frac{M_1^2}{L_2'} \right)$$

and the reactance is

$$\text{III-74} \quad X_{sc} = \omega \left(L_1 - \frac{M_1'^2}{L_2'} \right)$$

Exciting the secondary and shorting the primary would give the following values referred to the primary:

$$\text{III-75} \quad l_{sc} = L_2' - \frac{M_1'^2}{L_1}$$

and

$$\text{III-76} \quad X_{sc} = \omega \left(L_2' - \frac{M_1'^2}{L_1} \right)$$

Case III. Primary and secondary excited in such a manner that primary and secondary ampere turns are equal if the exciting current is neglected.

Physically this is easily accomplished by varying the applied

voltages so that $I_1 = I_2' = I$

under these conditions

$$\text{III-77} \quad E_1 = J\omega\bar{\psi}_1 = J\omega(L_1 I - M' I)$$

$$\text{III-78} \quad E_2' = J\omega\bar{\psi}_2 = J\omega(L_2' I - M I)$$

Since the mmf. of one winding equals that of the other and the geometrical configuration of the magnetic circuit is the same for each winding, the net mutual flux is zero. Thus, the nonuseful linkage is the sum of the linkages of each winding.

$$\text{III-79} \quad \psi_1 + \psi_2' = (L_1 + L_2' - 2M')i$$

The leakage inductance and leakage reactance are then respectively:

$$\begin{aligned} \text{III-80} \quad l_B &= L_1 + L_2' - 2M \\ &= (L_1 - M') + (L_2' - M') \\ &= l_{oc \text{ primary}} + l_{oc \text{ (secondary)}} \end{aligned}$$

$$\text{and III-81} \quad X_B = \omega(L_1 + L_2' - 2M')$$

Leakage reactance when defined in this manner is commonly called "bucking reactance".

$$\text{Since} \quad L_1 = 0.4\pi N_1^2 \rho_1 \cdot 10^{-8}$$

$$\text{and} \quad L_2' = 0.4\pi N_2^2 \rho_2 \cdot 10^{-8} \left(\frac{N_1}{N_2}\right)^2 = 0.4\pi N_1^2 \rho_2 \cdot 10^{-8}$$

$$\text{and} \quad \rho_1 \approx \rho_2, \quad \text{then} \quad L_1 \approx L_2'$$

$$\text{and III-82} \quad l_B = 2(L_1 - M')$$

$$\text{III-83} \quad l_B \approx 2 l_{oc}$$

Therefore, the bucking reactance is nearly twice that of the open circuit reactance. This variation may be accounted for by the difference in the mmf. across the leakage path. In the case of the open circuit condition the mmf. varies nearly linearly from a maximum value at the primary leg of the core to zero at the secondary leg of the core. Now in the case of the bucking condition, equal mmf. is supplied by each leg. As before, the mmf. of any one leg drops linearly and reaches zero at the other leg. However, since both are linear functions, the sum at any point is equal to that at any other point. Consequently, the average mmf. is approximately twice the value obtained in the open circuit case.

In order to compare the value of short circuit reactance with the bucking reactance the following manipulation is done.

From equation III-70, $I'_2 = \frac{M'}{L'_2} I_1$ since $I'_2 = I_1$ if the magnetizing current is neglected, then $M' = L'_2$. If equation III-73 is subtracted from equation III-80 the difference in the leakage inductance is obtained.

$$\begin{aligned} l_B - l_{sc} &= (L_1 + L'_2 - 2M') - \left(L_1 - \frac{M_1^2}{L'_2} \right) \\ &= \frac{L_2'^2 - 2M'L'_2 + M'^2}{L'_2} \\ \text{III-84} \quad &= \frac{(L'_2 - M')^2}{L'_2} \end{aligned}$$

and if the magnetizing current is small compared to the load current then:

$$l_B - l_{sc} = 0$$

Summarizing the resultant facts:

1. The leakage inductance may vary in a ratio between 1:1 and 2:1 depending upon whether the load is an open circuit, partially loaded, or short circuited.
2. The value of bucking reactance is practically equal to that of short circuit reactance provided the magnetizing current is small compared to the load current.
3. For purposes of visualization the flux distribution under short circuit conditions should be that shown in Figure III-5.

Case IV. Primary excited with a suddenly applied d.c. voltage and secondary short circuited.

The differential equation governing the circuit is

$$\text{III-85} \quad E U(t) = r_1 i_1 + \frac{d\psi}{dt} = r_1 i_1 + \frac{d}{dt}(L_1 i_1 - M' i_2')$$

$$\text{III-86} \quad 0 = r_2' i_2' + \frac{d\psi_2'}{dt} = r_2' i_2' + \frac{d}{dt}(L_2' i_2' - M' i_1')$$

where $U(t)$ is the unit step function which has the value 0 when approached from the negative time direction, and has the value +1 anytime after $(0+)$ and also at zero when approached from the positive time direction.

Integrate both equations with respect to time.

$$\text{III-87} \quad \int_0^t E U(t) dt = \int_0^t r_1 i_1 dt + \int_0^{\psi_1} d\psi_1$$

$$\text{III-88} \quad 0 = \int_0^t r_2' i_2' dt + \int_0^{\psi_2'} d\psi_2'$$

By letting $t \rightarrow$ zero from the positive direction, then in the limit the equation III-88 becomes zero. Thus

$$\begin{aligned} 0 &= \int_0^{\psi_2'} d\psi_2' \\ \text{III-89} \quad &= \psi_2' = L_2' i_2' - M i_1 \end{aligned}$$

$$\text{therefore} \quad \text{III-90} \quad i_2' = \frac{M}{L_2'} i_1$$

when t is infinitesimally small. Substituting back in equation gives:

$$\text{III-91} \quad E U(t) = r_1 i_1 + \left(L_1 - \frac{M^2}{L_2'} \right) \frac{di_1}{dt}$$

for the first short interval of time. As the interval becomes zero when time is approached from the positive direction the expression is exact. However, for a short interval after $t = 0$ the expression is approximate. If r_2' is large, it reduces the time interval through which the approximation is very close to the actual value. Equation III-91 shows that during the first short interval the effective inductance with suddenly applied d-c voltage is identical to the short circuit inductance with a. c., both under the condition of the secondary short circuited.

Equation III-89 may be physically justified by realizing that the sudden application of the d-c voltage causes an exponential rise of primary current. Simultaneously, the secondary current also builds up exponentially, thereby attempting to keep the secondary linkage zero.

Short circuit problems are often analyzed by the constant flux linkage of R. E. Doherty. This theorem states that the total linkage in any closed electrical circuit cannot change instantly. A "closed

circuit" is defined as one which involves no infinite voltages or resistances but it may contain any number of finite resistances, inductances (including mutual inductance), and the inductance may vary as a function of time. By applying Kirchhoff's law to instantaneous voltages, then the rate at which the total linkage varies is proportional to the difference between the applied emf. and the iR drop.

The previous discussion shows that when a closed winding is magnetically coupled to another circuit and a d-c voltage or a-c suddenly applied, the flux linkages of the closed winding remains practically constant, and all of the new flux links the excited winding. Since the leakage path between the two windings (air path) has very low permeance, the initial effective inductance of the excited winding is very low, as verified mathematically to be $(L_1 - \frac{M_1^2}{L_2'})$. If the magnetizing current were neglected, the quantity in the parentheses would become zero.

Heretofore, the subject has been confined to static cases, i.e. no motion between windings. The concepts previously developed will be broadened so as to pertain to cases involving motion between windings, i.e. that relating to rotating machinery.

The subsequent discussion will be confined to machines having symmetrical 3 - phase armature windings wherein the effects of saturation, hysteresis and eddy current losses will be neglected. Symmetry of the field winding and of the field structure about the center lines of the poles, direct axis, and also about the center line midway between the poles, quadrature axis, is assumed.

Armature Leakage Reactance X_1

Suppose that three phase currents of fundamental frequency flow in the armature with normal phase rotation, i.e. positive sequence, as a

result of applying a voltage to the armature terminals. These currents produce a flux wave composed of the fundamental and also of harmonic components due to the finite number of slots. Accordingly, the fundamental flux component rotates forward at synchronous speed, the fifth harmonic rotates backward, the seventh harmonic rotates forward, etc. Since these harmonics travel at speeds different from that of the rotor, their interaction with the varying permeance of the rotor gives rise to flux harmonics of various orders. The effect of a solid cylindrical rotor is to allow a flow of currents which tends to reduce the magnitudes of the flux components. Obviously, certain of these flux harmonics will induce voltages of fundamental frequency in the armature. However, these effects, due to what is known as differential leakage flux linkage, are included in the armature leakage reactance.

Additional linkages of the armature are due to slot flux and end flux in the winding. Therefore, the total armature leakage flux linkage consists of the sum of the differential, slot, and end winding linkages. The armature leakage inductance in henrys is obtained by multiplying the ratio of the linkage in one phase to the armature phase current producing it by 10^{-8} .

Direct Synchronous Reactance X_d

Again the assumption is made that such a voltage is applied to the armature as to cause a flow of fundamental frequency currents in the positive sequence direction. The major component of armature linkage is due to the fundamental component of the air gap flux which exists in addition to the leakage flux linkage. This component differs from the latter in that it is greatly affected by the position of the field structure.

Two particular cases may be examined. The first is that in which the fundamental component of armature mmf. is directly in line with the poles of the field structure. In this case maximum permeance is presented to the mmf.; consequently, maximum total armature linkage per armature ampere results. For this condition the ratio of the linkages in one phase to the current in that phase multiplied by 10^{-8} gives the direct synchronous reactance per phase, in ohms. The effects of armature leakage reactance is included in this definition.

The meaning of direct synchronous reactance may be clarified somewhat by an examination of the physical functioning of the machine. If the flux of only one phase is investigated, it will be found to be stationary in space, but pulsating at the angular frequency of the current which produces it. The number of flux linkages existing at any instant of time, depends upon the position of the salient pole rotor for the same instant of time. When the current reaches a maximum at the same instant that the centerline of the rotor pole coincides with the centerline of the phase winding, the maximum number of linkages occur; at this instant the magnetic circuit has maximum permeance. Now suppose that the current reached a maximum when the centerlines of the rotor and of the winding were not coincident, then the reactance would be less than that previously obtained since fewer flux linkages would occur for the same maximum armature current due to the reduced magnetic permeance at that instant of time. From this it may be seen that the value of the reactance depends upon the relative position of the rotor with respect to the mmf.

For experimental purposes it is difficult to rotate the field structure so that centerlines of the poles are always in line with the axis

of the rotating armature mmf. One method which may be used to obtain the direct axis reactance is to short circuit the machine and find the ratio of the phase voltage to phase current. The reason for the correctness of this procedure is that under short circuit conditions the current flowing is practically all reactive and therefore, the armature mmf. directly opposes that of the rotor poles tending to demagnetize them. Of course, in this method the machine must be driven by a mechanical source of power.

By neglecting saturation the flux linkage in any one circuit is a linear function of the magnitudes of the currents existing in every other winding of the machine; thus, the principle of superposition may be used to determine the linkage. The total linkage of a given circuit is therefore the sum of that due to its own current plus that due to currents flowing in the remaining windings.

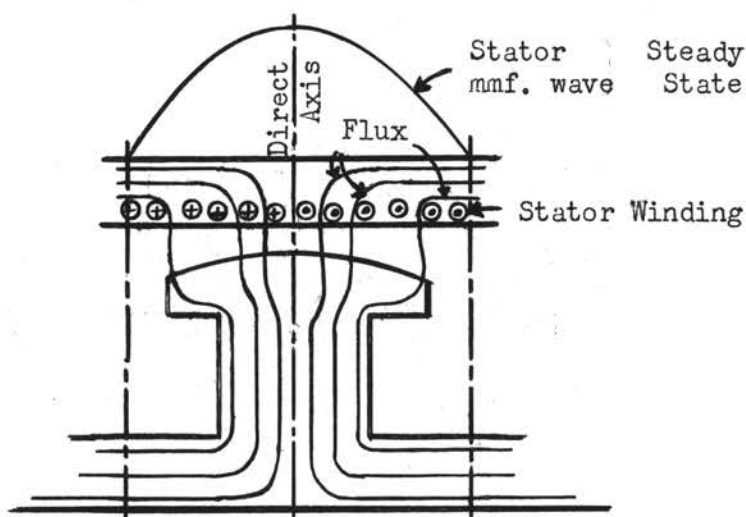


FIGURE III-6

Direct synchronous reactance flux paths.

Under symmetrical short circuit conditions the terminal voltage is zero. If resistance drop is neglected the net armature linkage must be zero. Under this condition the linkages produced by the armature current is equal and opposite to that of the field. If only the field current were acting (open circuit) a certain terminal voltage would exist. Now if the armature currents were acting alone, the same value of linkage but of opposite direction would result. The voltage which must be applied to produce the armature currents would be exactly the same as that under open circuit conditions. The definition of X_d gives it as the ratio of the terminal phase voltage, which would produce the armature currents alone, to the armature phase current. From this and the previous discussion it may be deduced that

$$X_d = \frac{E_{\text{open circuit air gap line}}}{I_{\text{short circuit}}} \text{ ohms}$$

Quadrature Synchronous Reactance X_q

Again it will be assumed that positive sequence steady-state currents are flowing in the armature and that the unexcited field structure is rotating at synchronous speed. However, now the centerline of the interpolar space coincides with the peaks of the rotating mmf. wave. The magnetic circuit now has minimum permeance and the armature linkage will be a minimum for any position of the poles. Refer to Figure III-7 to observe the flux paths. Multiplying the armature linkage per ampere by $\omega 10^{-8}$ gives the quadrature synchronous reactance, X_q , in ohms. Again this reactance includes the leakage reactance. When the rotors are of non-salient pole construction $X_d = X_q$.

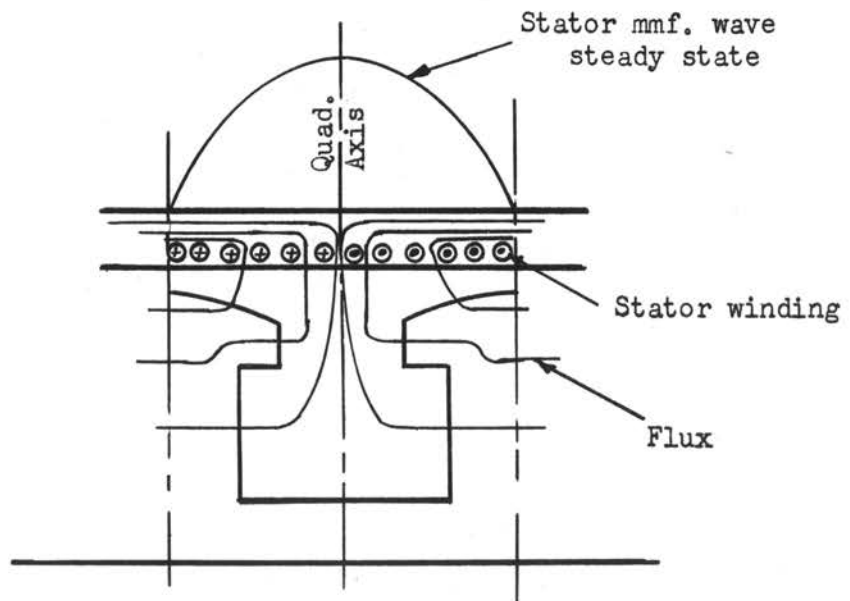


FIGURE III-7

Quadrature synchronous reactance flux paths.

PART V

Mathematical Analysis of the Three-Phase Reluctance Motor

In Chapter I it was mentioned that a d-c excited polyphase synchronous motor would continue to run if the excitation were reduced and finally entirely removed, i.e. operate on the reluctance principle. With this in mind, a logical method for analyzing the three-phase reluctance motor would be to analyze it as if it were operating as a three-phase synchronous motor in which the excitation had dropped to zero. It is for this analysis that the quantities were developed in the preceding parts of this chapter.

Since the reluctance motor has a variation in the gap reluctance, methods of analysis for non-salient pole machines do not give accurate results when applied to salient pole ones. As previously discussed, the magnetic permeance has a maximum value when the centerline of the rotor pole coincides with the peak of the rotating mmf. and has a minimum when the centerline midway between the rotor poles coincides with the peak of the rotating mmf. From this it would appear possible to analyze the performance of the motor in terms of the direct axis reactance and of the quadrature axis reactance. Although Blondel is credited with the two reaction theory, it was the extension of it by Doherty and Nickle which made it applicable to the salient pole synchronous motor.

Consider the synchronous motor vector diagram as shown in Figure III-8.¹ This is drawn for leading power factor on a per phase basis with the armature resistance neglected.

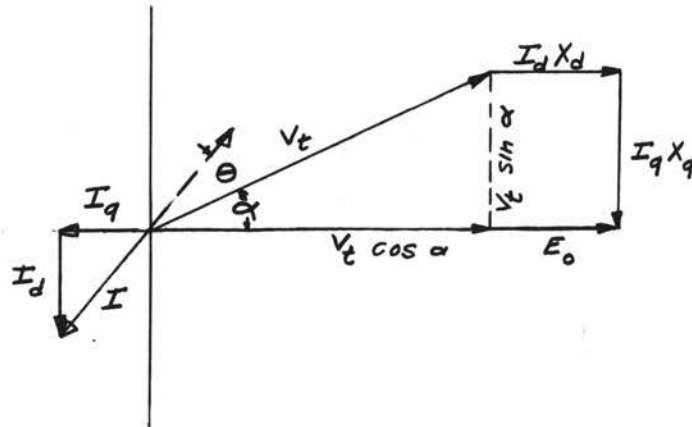


FIGURE III-8

Synchronous Motor Vector Diagram

The torque angle expressed in electrical degrees is identical to the angle between the terminal voltage V_t and the induced voltage E_0 expressed in the same units. The components of line voltage which are in-phase and in-quadrature with the induced voltage are $V_t \cos$ and $V_t \sin$ respectively.

$$\text{III-92} \quad P_{in} = V_t I \cos \theta \left] \begin{matrix} V_t \\ I \end{matrix} \right.$$

$$= V_t I \cos [\alpha - (\theta + \alpha)]$$

$$= V_t I [\cos \alpha \cos (\theta + \alpha) + \sin \alpha \sin (\theta + \alpha)]$$

$$\text{III-93} \quad = (V_t \cos \alpha) I \cos (\theta + \alpha) + (V_t \sin \alpha) I \sin (\theta + \alpha)$$

¹The following derivation is taken largely from Puchstein, A. F. and Lloyd, T. C., Alternating Current Machines, p. 435.

$$\text{III-94} \quad P_{in} = (V_t \cos \alpha) I_q + (V_t \sin \alpha) I_d$$

Further examination of Figure III-8 shows

$$\text{III-95} \quad V_t \cos \alpha = E_0 - I_d X_d$$

$$\text{or} \quad I_d = \frac{E_0 - V_t \cos \alpha}{X_d}$$

$$\text{and} \quad \text{III-96} \quad V_t \sin \alpha = I_q X_q$$

$$\text{or} \quad I_q = \frac{V_t \sin \alpha}{X_q}$$

Substituting these values in equation III-94 gives

$$\text{III-97} \quad P_{in} = V_t \cos \alpha \frac{V_t \sin \alpha}{X_q} - V_t \sin \alpha \frac{E_0 - V_t \cos \alpha}{X_d}$$

$$\text{III-98} \quad = \frac{V_t E_0}{X_d} \sin \alpha - \frac{V_t^2 (X_d - X_q)}{2 X_d X_q} \sin 2\alpha$$

The developed power is equal to the input power minus the copper losses. This becomes

$$\begin{aligned} \text{III-99} \quad P_{der} = & \frac{V_t E_0}{X_d} \sin \alpha + \frac{V_t^2 (X_d - X_q)}{2 X_d X_q} \sin 2\alpha + \\ & -(I_d^2 + I_q^2) r_e \end{aligned}$$

An examination of equation III-99 shows that the torque does not vary simply as the sine of the torque angle but has in addition a function which is the sine of twice the torque angle. Thus, the salient pole machine develops more torque per degree than the non-salient pole one does in the normal operating range.

Since the field excitation is zero in the three-phase reluctance motor the induced voltage E_0 becomes zero and equation III-99 becomes:

$$\text{III-100} \quad P_{\text{dev}} = \frac{V_t^2 (X_d - X_q)}{2X_d X_q} \sin 2\alpha - (I_d^2 + I_q^2) r_e$$

In most machines there is only a few per cent of difference between the developed power and the input power; the last term may be deleted without serious error. Thus, the final expression for developed power in the three-phase reluctance motor is

$$\text{III-101} \quad P_{\text{dev}} = \frac{V_t^2 (X_d - X_q)}{2X_d X_q}$$

CHAPTER IV

Experimental Analysis of the Three-Phase Reluctance Motor

PART I

Determination of X_d and X_q

An experimental analysis of the three-phase reluctance motor was conducted for the purpose of verifying the theoretical equations which were derived in Chapter III.

Accordingly, tests were run on a three-phase a-c salient pole Westinghouse machine No. 4887398. This machine normally operates as an a-c generator and is direct coupled to a Westinghouse d-c machine. However, in this case, the a-c machine was operated as a reluctance motor and the d-c machine was used as a generator for loading it.

Since it was necessary to know the direct axis reactance and the quadrature axis reactance of the machine under test, some means must be used to determine it experimentally. The direct axis reactance could be determined by the method developed in Part IV of Chapter III if the saturation curve and synchronous impedance curve of the machine were known. However, since this data was not available, and also since the quadrature axis reactance could not be obtained with such data, a different approach was taken.

Consider the instant at which the centerline midway between the rotor poles is coincident with the centerline of an armature phase whose current is at a maximum. At this instant, the minimum reactive voltage is induced in the phase. Any other rotor position would cause a larger induced voltage which would thereby reduce the phase current. In fact, the maximum induced voltage would occur when the centerline of the poles was coincident with the centerline of the phase. Since X_d and X_q

are taken with the field structure in a symmetrical position with respect to the rotating mmf., there is no tendency for it to turn in either direction. Consequently, no power is transferred across the gap; therefore, the currents are purely reactive and it is correct to define a reactance for each case as the ratio of total voltage to total current.

Mechanically, it is difficult to rotate the field structure so that either the direct axis or quadrature axis is directly in line with the armature mmf. since any slight deviation from the symmetrical position will result in a torque which will tend to make the deviation even greater. A method for overcoming this drawback is to mechanically drive the unexcited rotor in the synchronous direction but at a speed slightly less than the rotating armature mmf. while positive phase sequence voltages are impressed on the armature terminals. Thus, for the six pole machine under test, every time the rotor slips one revolution with respect to the rotating armature mmf. the rotor is six times in the direct axis position and six times in the quadrature axis position. Thus, the current is modulated at slip frequency, being a maximum when the direct axis is in that position. Also the applied voltage will probably be modulated at slip frequency as a result of reactance in the supply line.

The higher the value of slip, the fewer undulations there are to a complete cycle of events, i.e. from the time the rotor is in the direct axis position, then quadrature axis position, and then back to the direct axis position. Hence, if a voltmeter and ammeter are used for measuring purposes, since they tend to indicate an average value where the magnitude of the waveform is varying, a low value of slip must be used. However, when a low enough value is reached to give satisfactory meter readings,

the rotor locks in, thereby destroying the test. To overcome this difficulty higher values of slip were used and the instantaneous values of voltage and current recorded by means of oscillograms.

Figure IV-1 shows photographs of the waveforms of the current and voltage under test. Calibrations were obtained by applying a known voltage and current to the same elements of the oscillograph as previously used, and recording them on the film. Notice the variations due to the interaction of the flux harmonics on the slots and rotor saliency. In particular the distortions are in symmetrical positions with respect to either the direct axis or quadrature axis position.

From these oscillograms maximum and minimum rms. phase voltages of 78 and 69 volts were obtained. Similarly the maximum and minimum phase currents were found to be 12.0 and 6.8 rms. amperes respectively. Using these values the direct axis reactance and quadrature axis reactance were computed as shown below.

$$\begin{aligned} X_d &= \frac{\text{Maximum volts/phase}}{\text{Minimum current}} \\ &= \frac{78}{6.8} \\ &= 11.47 \text{ ohms} \end{aligned}$$

$$\begin{aligned} \text{and } X_q &= \frac{\text{Minimum volts/phase}}{\text{Maximum current}} \\ &= \frac{69}{12.0} \\ &= 5.72 \text{ ohms} \end{aligned}$$

Upper oscillogram represents the phase current which has a maximum peak value of 12 amperes and a minimum peak value of 6.8 amperes.

Lower oscillogram represents the phase voltage which has a maximum peak value of 78 volts and a minimum peak value of 69 volts.

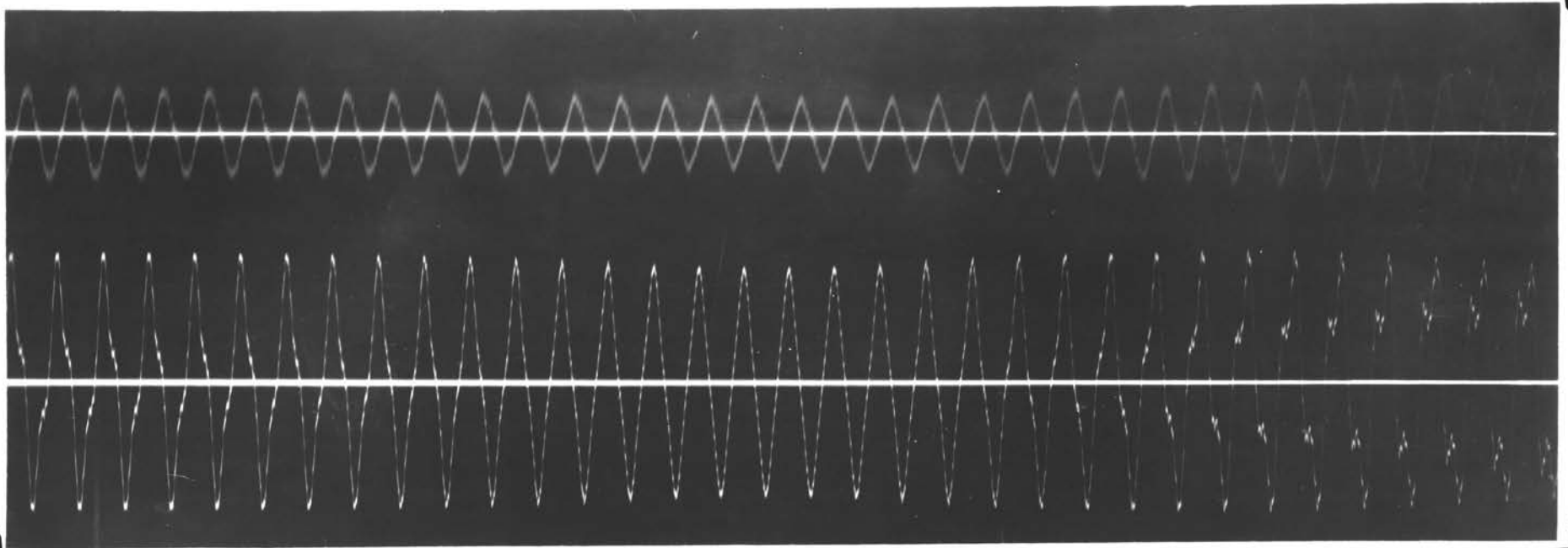


Figure IV-1

PART II

Reluctance Motor Performance Test

The performance of the Westinghouse a-c machine operating as a reluctance motor was determined under load conditions in the following manner. Since the d-c machine was direct-coupled to the a-c machine by operating the former as a motor it was able to start and to bring the reluctance motor up to synchronous speed. Of course, it was necessary that the direction of rotation of the d-c machine and the reluctance motor be ascertained to be the same. This was accomplished by connecting phasing lamps between the terminals of the reluctance motor and the a-c line and applying a d-c voltage to the field circuit, i.e. operating as an a-c generator. With the particular type of lamp connection used, if all lamps went on and off together the phase rotation was correct, if not, two of the a-c input lines were interchanged, thereby enabling all the lamps to go on and off simultaneously.

After checking the phase rotation, the input watts, line current, phase voltage, line voltage, and torque angle were recorded as the d-c generator load was increased by reducing the load resistance. These results with the exception of the torque angle are listed in table IV-1. . The torque angle was obtained by rigidly fastening a circular sheet of stiff paper to the reluctance motor housing and placing a horizontal white line on the circular pulley connecting the reluctance motor with the d-c generator. The light from a stroboscope excited from the same power source as the a-c motor showed the white line stationary in space. Thus at zero d-c generator load the position of the white line as indicated by the stroboscope was marked by a fine pencil on the white paper.

Each time the load was increased the white line assumed a new position and this was again marked.

The difficulty of the test was in determining the rotor position at zero mechanical load, since even when the d-c generator output was zero the reluctance motor was considerably loaded due to rotational losses. Thus the true rotor position for any given load was that indicated on the paper plus the angle from zero mechanical load to that obtained with only the rotational losses present, i.e. with zero d-c generator load. This was obtained by plotting the increase in output power from one load position to the next larger divided by the change in the accompanying torque angle versus the output power for the first load position. This is equivalent to plotting the slope of the curve of output power versus torque angle against output power. The results of this procedure are shown in Curve Sheet No. IV-1. By extending the curve, $\Delta P / \Delta \angle$ could be found for the output power corresponding to the rotational losses only, 104.2 watts, and from it could be determined $\Delta \angle$ corresponding to the change in output power from zero mechanical output to 104.2 watts mechanical output. This value of 1.16 was then added to all the values indicated on the white paper to give the value of torque angle from the zero mechanical load position. The individual values calculated are shown in Table IV-3.

Since the motor operated at constant speed, the rotational losses were assumed constant throughout the test. They were obtained by using the d-c machine to drive the a-c machine and noting the armature input current and voltage and also its resistance. The calculations are as follows:

$$\begin{aligned}
 \text{Rotational losses} &= V_a I_a - I_a^2 R_a - 2 I_a^2 \\
 &= 232 \times \frac{8.5}{5} - 8.5^2 \times .876 - 2 \times 8.5^2 \\
 &= 313.8 \text{ watts}
 \end{aligned}$$

CURVE SHEET No IV-1

PLOT OF $\Delta P/\Delta L$ VERSUS OUTPUT
POWER FOR DETERMINING THE TRUE
TORQUE ANGLE OF WESTINGHOUSE
MACHINE NO. 4,887,398

$\Delta P/\text{PHASE}$
 ΔANGLE

X - KNOWN POINTS
O - POINT TO BE DETERMINED

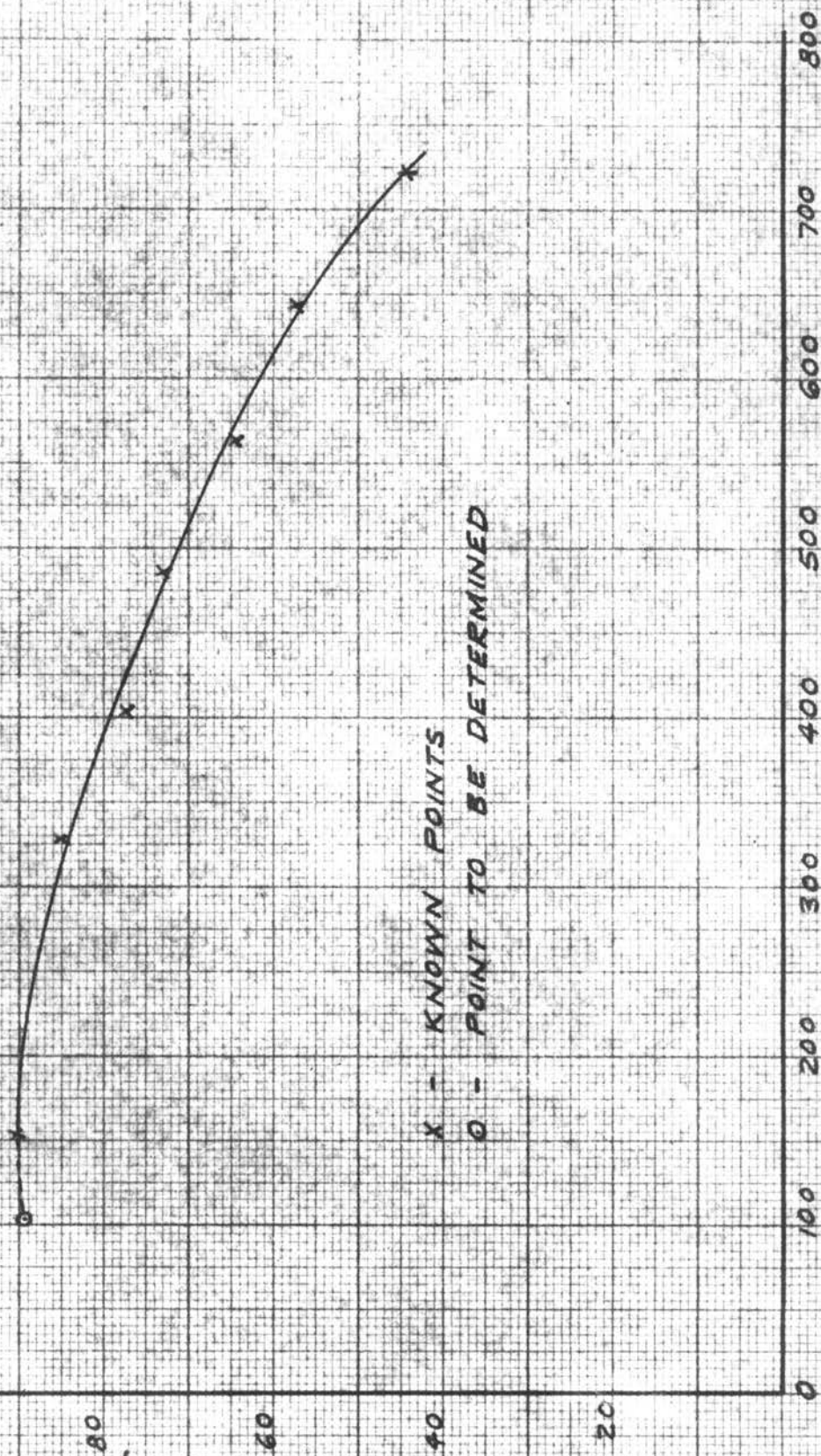


TABLE IV-1

Reading	Input Reluctance Motor - Non excited									D-C Generator Output	
	W_1 Kilo- watts	W_2 Kilo- watts	I_1 Amperes	I_2 Amperes	I_3 Amperes	V_{1-3} Volts	V_{1-n} Volts	V_{2-n} Volts	V_{3-n} Volts	V_a Volts	I_a Amperes
1	.59	-.38	16.3	16.7	16.5	239	138	138	138	228	0
2	.61	-.365	16.4	16.9	16.6	239	138	138	138	226	3.5
3	.69	-.31	17.1	17.5	17.4	238	138	138	138	224	14.5
4	.735	-.29	17.6	18.0	17.8	238	138	138	138	224	19.5
5	.79	-.26	18.4	18.9	18.7	238	138	138	138	222	25.0
6	.85	-.25	19.4	19.8	19.7	238	138	138	138	222	30.0
7	.92	-.24	20.5	21.0	20.8	237	138	138	138	221	35.0
8	1.05	-.26	23.3	23.6	23.4	237	138	138	138	219	40.0

True a-c kilowatts equals $(W_1 - W) \times 4$.

True d-c generator amperes equals I_a divided by 5.

Synchronism finally lost at reading 8.

Of course, the above rotational losses are the combined losses of the two machines.

Adding the rotational losses to the d-c generator output gives the total output of the reluctance motor. This is plotted versus the true torque angle on Curve Sheet No. IV-2.

In Chapter IV, Part V, the theoretical equation developed for predicting the performance of the three-phase reluctance motor was

$$P_{\text{dev}} = \frac{V_t^2 (X_d - X_q)}{2 X_d X_q} \sin 2\alpha$$

where V_t , α , X_d , and X_q are the line voltage, torque angle, direct axis reactance, and quadrature axis reactance respectively.

Substituting the values of V_t , X_d , and X_q for the particular machine under test, gives

$$\begin{aligned} P_{\text{dev}} &= \frac{138^2 (11.47 - 5.75)}{2 \times 11.47 \times 5.75} \sin 2\alpha \\ &= 827 \sin 2\alpha \end{aligned}$$

Table IV-6 shows the values of $\sin 2\alpha$ and the developed power per phase with various assumed values of α . Reference to Curve Sheet No. IV-2 will show the calculated developed power per phase plotted versus the torque angle α .

Using the average of the three line currents and $\cos \theta$ as determined by the power factor previously calculated, made it possible to plot the component of current which was in phase with the phase voltage as well as the component which was out of phase. Table IV-5 shows the computed values, and Curve Sheet No. IV-4 shows the in-phase component plotted versus the out-of phase component.

CURVE SHEET No. 2

TORQUE ANGLE CHARACTERISTIC
OF 3Φ WESTINGHOUSE RELUCTANCE
MOTOR

α - TRUE TORQUE ANGLE - ELECT. DEGREES

THEORETICAL
EXPERIMENTAL

OUTPUT POWER - WATTS/PHASE

800

700

600

500

400

300

200

100

0

30

25

20

15

10

5

0

TABLE IV-2

Input Reluctance Motor - Non Excited

Reading	Kilo-watts Total	Kilo-watts Phase	$V_1 - nI_1$ Volt Amperes Phase	$V_2 - nI_2$ Volt Amperes Phase	$V_3 - nI_3$ Volt Amperes Phase	V I Total Volt Amperes	V I Phase Average Volt Amperes	P. F.	* Angle Mech. Degrees
1	.84	.28	2250	2280	2305	6835	2280	.123	1.16
2	.98	.327	2260	2330	2290	6880	2290	.1425	1.75
3	1.25	.506	2360	2515	2400	7275	2420	.209	3.77
4	1.78	.594	2430	2483	2460	7373	2460	.2415	4.77
5	2.12	.707	2540	2610	2580	7730	2580	.274	5.90
6	2.40	.800	2680	2730	2720	8130	2710	.295	7.10
7	2.72	.908	2830	2900	2870	8600	2870	.316	8.56
8	3.16	1.052	3220	3260	3270	9750	3250	.324	10.35

*Torque angle indicated from the zero mechanical and electrical output rotor position; not the value recorded during the test.

CURVE SHEET NO 3

POWER FACTOR AND EFFICIENCY
CHARACTERISTICS OF WESTINGHOUSE
RELUCTANCE MOTOR #4887398

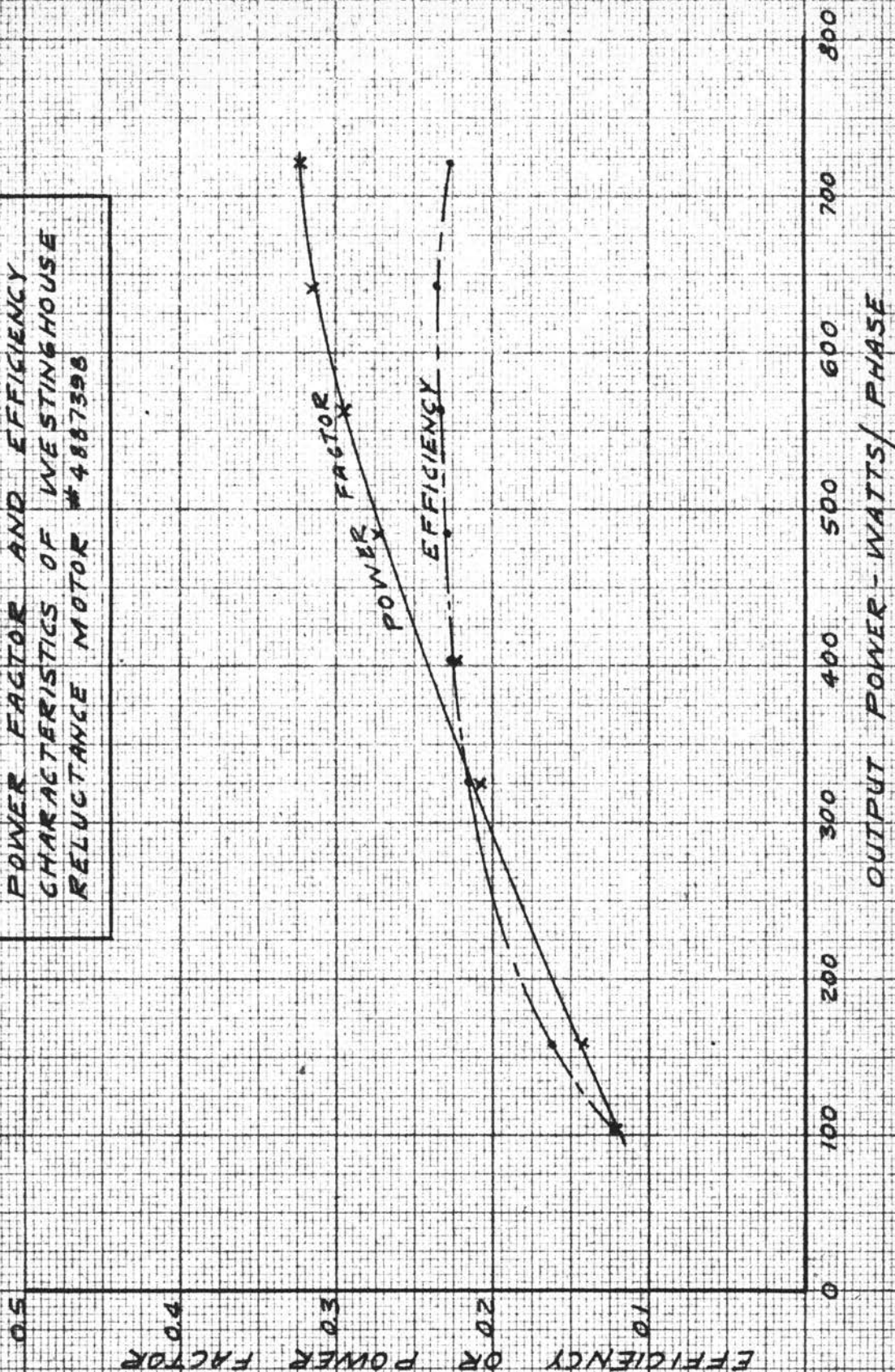


TABLE IV-3

A-C Reluctance Motor

Reading	Measured Torque Angle (Mech. degrees)	Total Output Power/Phase (Elect.-mech.) Watts	Δ Total Output Power/phase	Δ Torque Angle (Mech. degrees)	$\frac{\Delta P/\text{phase}}{\Delta \angle}$	True Torque Angle (mech. degrees)	True Torque Angle (Elect. degrees)
1	0.00	104	.			1.16	3.20
2	0.59	158	53.3	.59	90.4	1.750	5.2
3	2.55	326	168.	1.96	85.6	3.77	11.3
4	3.55	402	77.2	1.006	77.2	4.77	14.3
5	4.683	485	82.3	1.13	73	5.9	17.5
6	5.884	563	77.8	1.201	64.7	7.101	21.3
7	7.343	642	78.5	1.359	57.3	8.56	25.7
8	9.13	721	79	1.79	44.2	10.35	31.0

CURVE SHEET No. 4

INPUT LINE IN-PHASE COMPONENT
VERSUS OUT-OF-PHASE COMPONENT
FOR 3Ø WESTINGHOUSE RELUCTANCE
MOTOR

X EXPERIMENTAL
O SECOND DEGREE
EQUATION POINTS

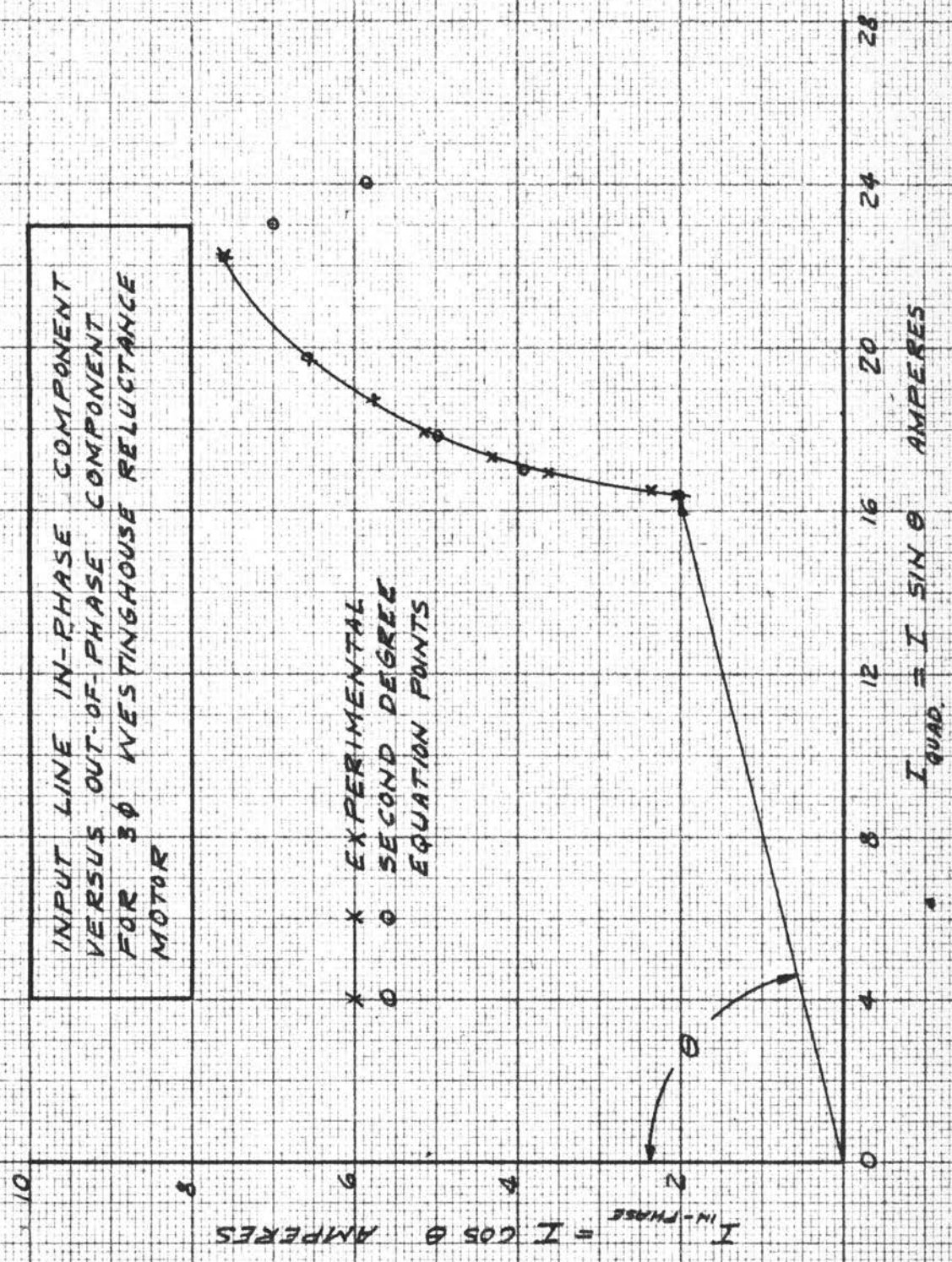


TABLE IV-4

D. C. Generator						Combined Rotational Losses of Motor + Generator	Reluctance Motor		
Reading	Watts Load Rack	I_a Amperes Corrected	$I_a^2 R_a$ Loss Watts	$2I_a$ Watts	Total Watts Elect.		Total Output Power-Watts (Elect.+Mech.)	Total Output Power/phase Watts (Elect.+Mech.)	Efficiency
1	0	0.0	0.0	0.0	0.0	313.8	313.8	104.2	.124
2	158	0.7	0.43	1.4	159.8	313.8	473.6	157.6	.161
3	650	2.9	7.35	5.8	663.1	313.8	976.9	326	.215
4	874	3.9	13.3	7.8	895.1	313.8	1208.9	403	.226
5	1110	5.0	21.9	10.0	1141.9	313.8	1455.7	485	.229
6	1332	6.0	31.5	12.0	1375.5	313.8	1689.3	564	.235
7	1554	7.0	42.9	14.0	1610.9	313.8	1924.7	643	.236
8	1776	8.0	56.1	16.0	1848.1	313.8	2161.9	722	.228

TABLE IV-5

Reading	I cos θ Amperes	I sin θ Amperes	I _{avg.}	P.F.
1	2.03	16.38	16.5	.123
2	2.37	16.45	16.63	.1425
3	3.62	16.95	17.33	.209
4	4.3	17.28	17.8	.2415
5	5.12	17.92	18.66	.274
6	5.78	18.72	19.6	.295
7	6.55	19.67	20.76	.3165
8	7.60	22.18	23.43	.324

TABLE IV-6
Theoretical Results

α Torque Angle (Elect. degrees)	$\sin 2\alpha$	$P_{\text{dev.}}/\text{Phase}$
0	0	0
2.5	.0872	72.3
5	.1736	143.7
10	.342	283
15	.500	413
20	.642	532
25	.766	634
30	.866	717
35	.939	777
40	.985	815
45	1.00	827
50	.985	815
55	.939	777
60	.866	717
70	.642	532

PART III

Comparison of Theoretical and Experimental Results

Reference to Curve Sheet No. IV-2 shows very good agreement between the experimental and theoretical results. For large values of torque angle, the experimental torque angle increased somewhat faster than did the theoretical value, finally causing a cross over of the two curves.

The experimental results of the in-phase versus out-of-phase line currents which are plotted on Curve Sheet No. IV-4 might have been expected to give the usual circle diagram. A closer examination would lead one to believe that it would more nearly coincide with the locus of an ellipse than a circle. Accordingly, it was decided to determine the mathematical equation of the curve. A second degree solution was used since it would enable one to determine by examination of the coefficients whether the locus was a circle ellipse, or something else; also this simplified the calculations as the work involved increases very rapidly with increase of equation degree.

A general second degree equation which fits any continuous smooth curve is

$$A + B I_q + C I_q^2 = I_{ln}$$

Two points on the extreme of the experimental curve and one approximately midway were selected for substitution in the previous equation.

This results in $A + B 16.38 + C 268.304,4 = 2.03$

$$A + B 17.8 + C 316.84 = 5.00$$

$$A + B 22.18 + C 491,952,4 = 7.60$$

The values of A, B, and C are found by determinants as shown below.

$$\begin{aligned}
 D &= \begin{vmatrix} 1 & 16.38 & 268.304,4 \\ 1 & 17.8 & 316.84 \\ 1 & 22.18 & 491.952,4 \end{vmatrix} \\
 &= \left[(8,756.752,7 + 5,189.839,2 + 5,950.991,5) - \right. \\
 &\quad \left. (4,774.818,3 + 8,058.180,3 + 7,027.511,2) \right] \\
 &= 36.073,6
 \end{aligned}$$

$$\begin{aligned}
 A \times D &= \begin{vmatrix} 2.03 & 16.38 & 268.3044 \\ 5 & 17.8 & 316.84 \\ 7.6 & 22.18 & 491.952,4 \end{vmatrix} \\
 &= \left[(17,776.208 + 39,442.777 + 29,754.957) - (36,296.219,2 + \right. \\
 &\quad \left. 14,265.847,7 + 40,290.901,5) \right] \\
 &= - 3,879.026
 \end{aligned}$$

$$A = \frac{- 3,879.026}{D} = \frac{- 3,879.026}{36.073,6}$$

$$= - 107.530,8$$

$$\begin{aligned}
 B \times D &= \begin{vmatrix} 1 & 2.03 & 268.3044 \\ 1 & 5 & 316.84 \\ 1 & 7.6 & 491.952,4 \end{vmatrix} \\
 &= \left[(2,459.760,0 - 643.185,2 - 2,039.113,4) - (1,341.522 - \right. \\
 &\quad \left. 2,407.984 - 998.662,5) \right]
 \end{aligned}$$

$$= 393.891,3$$

$$B = \frac{393.891,3}{D} = \frac{393.891,3}{36.073,6}$$

$$= 10.919$$

$$C \times D = \begin{vmatrix} 1 & 16.38 & 2.03 \\ 1 & 17.8 & 5.00 \\ 1 & 22.18 & 7.60 \end{vmatrix}$$

$$= \left[(134.280 + 81.90 + 45.025) - (36.134 + 124.488 + 110.900) \right]$$

$$= -9.317$$

$$C = \frac{9.317}{D} = \frac{9.317}{36.073,6}$$

$$= -.258,27$$

Therefore, the required equation is

$$I_{ln} = 107.530,8 + 10.919 I_q + 0.258,27 I_q^2$$

It will be noticed on Curve Sheet IV-4 that excellent agreement between the experimental curve and the circled points obtained from the developed equation is obtained. A mathematical manipulation can be done which will show that the curve does not fall into the class of circles or ellipses. However, this is more readily noted by simply observing how abruptly the theoretical points on the right of the experimental curve drop. Neither a circle nor an ellipse could take such a path.

Curve Sheet IV-1 shows excellent agreement between the theoretical and experimental values of torque angle versus power output. At large values of torque angle, the torque angle determined experimentally increased more rapidly than that obtained from the theoretical equation for a given power increase. This finally caused the curves to cross each other.

CONCLUSIONS

In the search for information regarding the three-phase reluctance motor, little was obtained. Possibly the reason for this is attributable to the superior performance, as pertaining to power factor and efficiency, of the three-phase d-c excited synchronous motor. The advantage of the reluctance motor is its ability to operate at synchronous speed and still not require a field winding or d-c power supply. With increase of motor size these advantages become proportionally less.

Since the exchange forces vary greatly in the different materials of the ferromagnetic class, it can be readily appreciated how the performance of the reluctance motor can be improved by the selection of material. Originally it was planned to analyze the motor quantitatively as a function of magnetic forces. However, this had to be abandoned due to the great complexity involved.

The loci of current vectors indicate that some curve other than a circle or ellipse results with increase of load. A great amount of work was done in attempting to determine the equation of the curve by assuming a third degree equation. Solution of these simultaneous equations became so tedious as to cause abandonment in favor of the simpler second degree equation. From the latter it would appear that the overall reactance of the machine varies as the sum of a first degree and second degree function with respect to rotor position.

Further research work could well be directed toward verifying the theoretical equation for predicting three-phase motor performance by experimental work on other motors, and to extend the concepts developed herein to the single phase reluctance motor.

BIBLIOGRAPHY

- Beweley, L. V. "Flux Linkages and Electromagnetic Induction in Closed Circuits." Transactions of American Institute of Electrical Engineers, 48 (1929), 327.
- Bozarth, R. M. "Present Status of Ferromagnetic Theory." Transactions of American Institute of Electrical Engineers, 54 (November, 1935), 1251.
- Cohn, George I. "Electromagnetic Induction." Electrical Engineering Transactions, 68 (May, 1949), 441.
- Electrical Engineering Staff, M.I.T. Magnetic Circuits and Transformers. New York: John Wiley and Sons, 1943.
- Hildebrand, F. B. Advanced Calculus for Engineers. New York: Prentice Hall Inc., 1949.
- Langsdorf, A. S. Theory of Alternating-Current Machinery. New York: McGraw-Hill Book Company, 1937.
- Page, Leigh Introduction to Theoretical Physics. New York: D. Van Nostrand Company, 1935.
- Prentice, B. R. "Fundamental Concepts of Synchronous Machine Reactance." Transactions of American Institute of Electrical Engineers. Vol. 56, (June, 1937).
- Puchstein, A. F. and Lloyd, T. C. Alternating-Current Machines. New York: John Wiley and Sons, 1942.
- Ricker, C. W. and Tucker, C. E. Electrical Engineering Laboratory Experiments. New York: McGraw-Hill Book Company, 1940.
- Shoults, D. R., Rife, C. J., and Johnson, T. C. Electric Motors in Industry. New York: John Wiley and Sons, 1942.
- Skilling, H. H. Fundamentals of Electric Waves. New York: John Wiley and Sons, 1948.
- Trickey, P. H. "Performance Calculations on Polyphase Reluctance Motors." Transactions of American Institute of Electrical Engineers, 65 (April, 1946), 191.
- Veinott, C. G. Fractional Horsepower Electric Motors. New York: McGraw-Hill Book Company, 1939.

Thesis Title: Analysis of the Three-Phase Reluctance Motor

Name of Author: Elman R. Showers

Thesis Advisor: Charles F. Cameron

The content and form have been checked and approved by the author and thesis advisor. "Instructions for Typing and Arranging the Thesis" are available in the Graduate School office. Changes or corrections in the thesis are not made by the Graduate School office or by any committee. The copies are sent to the binding just as they are approved by the author and faculty advisor.

Name of Typist: Ruby Lee Knox